Nonlinear guided waves in planar structures

D. Mihalache
Institute of Atomic Physics, Bucharest, Rumania

R. G. Nazmitdinov and V. K. Fedyanin
Joint Institute for Nuclear Research, Dubna

R. P. Yang
Peking University, Peking, China

Fiz. Elem. Chastits At. Yadra **23**, 122–173 (January–February 1992)

A survey is given of propagation phenomena of nonlinear surface and guided waves through planar dielectric layered structures containing both Kerr-law and saturable media. The basic linear–nonlinear Schrödinger-like equation governing the amplitude dynamics of these waves is derived and solved by numerical methods. It is then used to discuss the physics of spatial soliton formation in nonlinear planar structures. A transfer-matrix formalism for obtaining the stationary field distribution and the rich structured nonlinear dispersion curve of nonlinear optical waves in periodic stratified dielectric structures is also presented. Some possible applications of these nonlinear guided waves to integrated all-optical devices are suggested.

INTRODUCTION

Investigations of the propagation of surface optical waves during recent years had led to the development of the theory of nonlinear surface waves in the case when one or several media in contact are characterized by a refractive index that depends on the intensity of the incident optical beam.[1–4] The profile of the optical field and the propagation constant β can also depend on the energy flux of the incident beam. From the beginning of the study of nonlinear surface waves[5–11] reflection and transmission phenomena have been analyzed, and also the condition of stability of optical beams incident on the interface of contiguous media.[12–14] Because of the potential practical application of nonlinear optical wave guides,[15–17] great attention has been devoted to the investigation of three-layer wave guides: linear dielectric (film) contiguous with nonlinear (Kerr) dielectrics or with nonlinear self-focusing (self-defocusing) dielectrics whose refractive indices possess the saturation property (Refs. 18–26); nonlinear (Kerr) or saturable self-focusing (self-defocusing) thin dielectric film contiguous with linear dielectrics.[27–30] The stability of the propagation of various nonlinear stationary waves was analyzed numerically in Refs. 31–33. Investigation of beam propagation in highly nonlinear wave guides makes it possible to understand the excitation conditions[34] and the effects of absorption and saturation in the emission of optical solitons.[35–37] There has been much theoretical and experimental study of the optical properties of linear[38–41] and nonlinear[42–47] multilayer media. Such structures play an important part in many applications, namely, layers with high optical reflectivity, multilayer thin films for magneto-optical information readout, and semiconducting superlattices for optoelectronics and optical processes. There has been much study of the properties of nonlinear optical waves guided by such structures, since, for example, semiconducting superlattices possess strong optical nonlinearity and are characterized by very short signal response times.[48,49] A nonlinear matrix formalism was considered recently in Ref. 49 for the case of a *TE* polarized optical field propagating in a multilayer linear–nonlinear system contiguous on both sides with linear media. In fact, already in Ref. 38 the transfer-matrix method (2×2 matrix) was used to make a detailed analysis of the properties of a multichannel dielectric wave guide contiguous on both sides with linear media and consisting of a set of dielectric layers with alternately varying refractive indices.

In this paper, we present an analytic study of the general case of an N-channel asymmetric wave guide contiguous on both sides with dielectrics of Kerr type. Using the transfer-matrix method,[50–52] we shall obtain exact solutions for a stationary distribution of the optical field and nonlinear dispersion curves in the case of a multilayer linear structure contiguous with a nonlinear medium.

The paper is organized as follows. Section 1 is devoted to the study of nonlinear optical waves in gradient (with varying refractive index) planar dielectric structures with both Kerr-law and saturable claddings. We discuss the main features of the propagation of nonlinear surface waves and nonlinear guided waves in planar layered structures. Nonlinear optical waves guided by self-focusing dielectric films of Kerr type surrounded by linear and nonlinear claddings are considered in Sec. 2. In Sec. 3, we analyze in detail the emission of spatial solitons from nonlinear planar structures. In Sec. 4 we investigate nonlinear surface and guided waves in finite and semi-infinite periodic step dielectric structures. At the end, we briefly summarize the conclusions.

This paper is a continuation of the analysis of the propagation of nonlinear optical waves in layered structures presented in Ref. 4.

 0090-4759/92/010052-24$04.00

1. NONLINEAR OPTICAL WAVES IN GRADIENT PLANAR DIELECTRIC STRUCTURES

Gradient optical wave guides with nonlinear (Kerr) cladding

We consider a gradient planar optical wave guide with nonlinear self-focusing cladding of Kerr type. The refractive index of the wave guide varies continuously in the film for $z \geqslant 0$ and has a fixed value n_s at $z=\infty$. We assume that the refractive index of the self-focusing Kerr substrate ($z \leqslant 0$) is given by

$$n^2(|\mathbf{E}|^2,z)=n_c^2+\alpha_c|\mathbf{E}|^2, \quad \alpha_c>0, \quad z\leqslant 0, \tag{1}$$

where n_c is the refractive index in the absence of a field, and α_c is the nonlinearity coefficient. We investigate in detail gradient wave guides whose refractive indices have Gaussian profile,

$$n^2(z)=n_s^2+(n_f^2-n_s^2)\exp[-(z/d)^2], \quad z>0, \tag{2}$$

and also exponential-like profiles of the form

$$n^2(z)=n_s^2+(n_f^2-n_s^2)\exp(-z/d), \quad z>0. \tag{3}$$

Here, d is the penetration depth, and n_f is the maximum value of the refractive index. The refractive-index profile of step form is defined as follows:

$$n^2=\begin{cases} n_f^2, & 0\leqslant z\leqslant d; \\ n_s^2, & z\geqslant d. \end{cases}$$

We assume that TE polarized stationary waves propagate along the x axis with z normal to the surface and are translationally invariant with respect to the y coordinate, i.e., are determined by a relation of the form

$$E_y(x,z,t)=\tfrac{1}{2}E_y(z)\exp[i(\beta k_0 x-\omega t)]+\text{c.c.} \tag{4}$$

Here, β is the effective refractive index (propagation constant), $k_0=\omega/c$ is the propagation constant in vacuum, and $E_y(z)$ is the actual value of the amplitude for the guided optical fields.

Maxwell's equations for x-independent guided waves (stationary field distribution) can be written in the form

$$\frac{d^2E}{dz^2}-k_0^2(\beta^2-n_c^2)E_y+\alpha_c k_0^2 E_y^3=0, \quad z<0; \tag{5}$$

$$\frac{d^2E}{dz^2}-k_0^2[\beta^2-n^2(z)]E_y=0, \quad z>0. \tag{6}$$

For waves characterized by the condition $E_y(z)\to 0$ as $|z|\to\infty$, i.e., for fields that decrease exponentially on either side of the boundary $z=0$, the solution of Eqs. (5) and (6) is well known:[53,55]

$$E_y(z)=(2/\alpha_c)^{1/2}q_c\{\cosh[k_0 q_c(z-z_c)]\}^{-1}, \quad z>0; \tag{7}$$

$$E_y(z)=AJ_{2\rho}[2V\exp(-z/2d)], \quad z>0, \tag{8}$$

where $J_{2\rho}$ is a Bessel function; $q_c=(\beta^2-n_c^2)^{1/2}$; $\rho=k_0 d(\beta^2-n_s^2)^{1/2}$ and $V=k_0 d(n_f^2-n_s^2)^{1/2}$.

For TE polarized waves, the field E_y and its derivative dE_y/dz are continuous functions along the interface $z=0$ of the linear and nonlinear media. These conditions lead to the following relationships between the integration constant z_c and A:

$$A=(2/\alpha_c)^{1/2}q_c[J_{2\rho}(2V)\cosh(k_0 q_c z_c)]^{-1}; \tag{9}$$

$$u=(k_0 d q_c)^{-1}\left[\frac{J_{2\rho+1}(2V)}{J_{2\rho}(2V)}V-\rho\right], \tag{10}$$

where $u=\tanh(k_0 q_c z_c)$. Note that $u=(k_0 q_c E_0)^{-1}\times(dE_y/dz)|_{z=0}$ and E_0, the value of the field on the surface $z=0$, is determined by

$$E_0(2/\alpha_c)^{1/2}q_c(1-u^2)^{1/2},$$

where $-1\leqslant u\leqslant 1$ and $u=1$ in the linear case ($\alpha_c=0$). The energy flux of the guided waves per unit length along the y axis is determined by means of the Poynting vector as follows:

$$P=\frac{1}{2}\int_{-\infty}^{\infty}\text{Re}(\mathbf{E}\times\mathbf{H}^*)_x dz=\frac{\beta}{2c\mu_0}\int_{-\infty}^{\infty}E_y^2(z)dz. \tag{11}$$

Finally, we have $P=P_c+P_f$,[53] where

$$P_c=2P_0\beta q_c(1-u); \tag{12}$$

$$P_f=4P_0\beta q_c^2 k_0 d(1-u^2)[J_{2\rho}^2(2V)]^{-1}\int_0^{2V}\frac{J_{2\rho}^2(x)}{x}dx. \tag{13}$$

Here, $P_0=(2a_c k_0)^{-1}(\varepsilon_0/\mu_0)^{1/2}$, where ε_0 and μ_0 are, respectively, the dielectric constant and the magnetic susceptibility in vacuum.

We consider the results of the calculation of the propagation constant as a function of the power of the energy flux in the case of an MBBA liquid crystal [$n_c=1.55$, $\alpha_c=n_c^2 n_{2c}(\varepsilon_0/\mu_0)^{1/2}=6.4\times10^{-12}$ (m/V)^2] deposited as cladding on a glass wave guide. Figure 1 shows the nonlinear dispersion curves for the case of a nonlinear self-focusing Kerr-law cladding for three profiles of the refractive index: exponential, Gaussian, and step type. In all the considered cases, the maximum value of the profile is at the surface $z=0$. The nonlinear TE_0 solution has a local maximum and exists in the region $\beta>n_f$ (in the linear case, the effective refractive index β is always less than the refractive index n_f of the thin guiding dielectric film). With increasing β, the maximum of the optical field is displaced from the region of the film into the nonlinear self-focusing cladding layer, and the TE wave is transformed into a nonlinear surface polariton guided by the interface.[5,7] The arrows in Fig. 1 indicate the transition points, when the maxima of the TE_0 and TE_1 waves are localized at the interface $z=0$ of the thin film and the nonlinear self-focusing cladding. It can be seen in Fig. 1 that the lowest maximum energy flux of the TE_0 wave corresponds to the exponential refractive index.

Gradient optical wave guides with saturable cladding

It is obvious that the form of the dielectric function is determined by the physical processes which are responsible for the particular type of nonlinearity. Kerr-type nonlin-

earity, which is expressed by a quadratic function of the local optical field, $\varepsilon^{NL}=\alpha_c|\mathbf{E}|^2$, arises because of electron, thermal, and other effects. In semiconducting materials in which nonlinearity due to absorption leads to the formation of excitons and plasmons, the form of the dielectric function is determined by the relation $\varepsilon^{NL}=\alpha_r|\mathbf{E}|^r$, where $1<r<2$ (Refs. 58 and 59). Moreover, in real materials it is impossible optically to vary to infinity the refractive index on account of the saturation effect. The limits of variation of the refractive index in the case of saturation, Δn_{sat}, vary from 10^{-1} to 10^{-4}. Saturation effects are important for gradient optical wave guides, since the interesting properties of nonlinear surface waves—those that depend on the energy flux—occur when the optically induced change in the refractive index, Δn_{sat}, is comparable with the refractive indices of the film, n_f, and the cladding, n_c, or is greater than their difference existing at small powers of the energy flux.

We model the dielectric function of the nonlinear self-focusing cladding layer in the form[4,23]

$$n^2(|\mathbf{E}|^2,z)=n_c^2+\frac{\varepsilon_{\text{sat}}\alpha_c|\mathbf{E}|^2}{(\varepsilon_{\text{sat}}+\alpha_c|\mathbf{E}|^2)},\quad \varepsilon_{\text{sat}}>0, \qquad (14)$$

where ε_{sat} is the saturation parameter. Note that the maximum change in the dielectric function is ε_{sat}, since in the limit $|\mathbf{E}|\to\infty$ we have $n^2\to\varepsilon_c+\varepsilon_{\text{sat}}$. For weak fields $\varepsilon\to\varepsilon_c+\alpha_c|\mathbf{E}|^2$; i.e., we have the case of an ordinary Kerr medium.

Figure 2 shows the energy flux as a function of the effective refractive index β for a nonlinear self-focusing saturable cladding with $\varepsilon_{\text{sat}}=0.1256$. For this value of ε_{sat}, it is only in the case of a step profile of the refractive index that we obtain a multiply valued solution for the TE_0 wave (continuous curve in Fig. 2). To demonstrate the effects of saturation, Fig. 3 shows the nonlinear dispersion curves for $\varepsilon_{\text{sat}}=0.0624$. In this case, the saturation effects not only change (for the TE_1 waves) but also even eliminate (for TE_0 waves) the characteristic nonlinear behavior of the dispersion curves.

In conclusion, we emphasize that the value of the local maximum of the energy flux of the TE_0 waves and the possible range of allowed values of the effective refractive index β can be controlled by an appropriate choice of the profile for the dielectric function of the cladding or of the characteristics that determine the saturation properties of the cladding.

If the fundamental TE_0 mode is used in the case of a nonlinear cladding of Kerr type, the exponential profile of the cladding is the best among all the possibilities that we have considered, since it enables one to operate with an optical beam of low power.

2. NONLINEAR OPTICAL WAVES GUIDED BY SELF-FOCUSING FILM DIELECTRICS OF KERR TYPE

The guiding properties of nonlinear self-focusing (self-defocusing) film dielectrics of Kerr type were discussed in

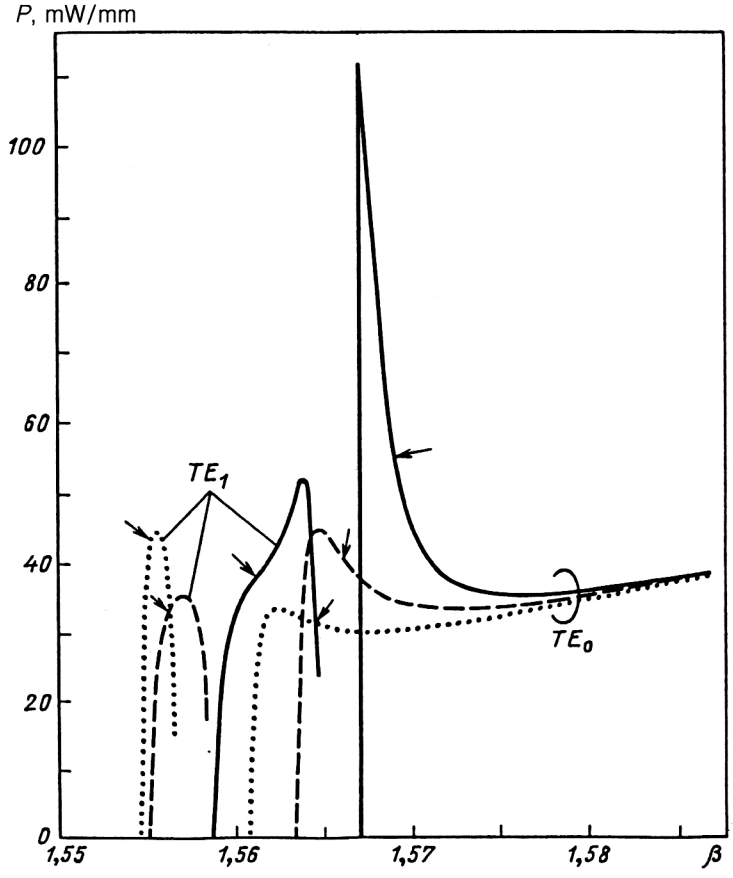

FIG. 1. Effective refractive index β as a function of the energy flux for a nonlinear cladding of Kerr type. The parameters in the calculation were as follows: $n_s=1.55$, $n_f=1.57$, $n_c=1.55$, $n_{2c}=10^{-9}$ m^2/W, $d=2$ μm, and $\lambda=0.515$ μm. The continuous curves are for a profile of step type, the broken curves for a profile of Gaussian type, and the dotted curves for an exponential profile.

detail in Refs. 27–31 and 60–63. In this section, we shall present the results of calculation of the stationary distribution of the optical field and the energy-flux-dependent refractive index for TE_m nonlinear optical waves guided by such dielectrics. The results of numerical investigation into the stability of the propagation of nonlinear guided waves have shown that the branch with negative slope of the dispersion curve is unstable. In addition, the basic characteristics of the propagation of nonlinear optical waves are significantly modified in the presence of linear absorption.

Propagation of nonlinear guided waves

We consider an asymmetric planar layered structure consisting of an optically linear medium (substrate) with dielectric constant ε_s in region I ($z<0$), a nonlinear self-focusing dielectric film of Kerr type of thickness d and dielectric function $\varepsilon=\varepsilon_f+\alpha_f|\mathbf{E}|^2$, $\alpha_f>0$, in region II ($0<z<d$), and a linear medium (cladding) with dielectric constant ε_c in region III ($z>d$).

Maxwell's equations for TE polarized waves propagating along the x axis with effective refractive index β have the form

$$\frac{d^2E_y^{\mathrm{I}}}{dz^2}-k_0^2(\beta^2-\varepsilon_s)E_y^{\mathrm{I}}=0, \quad z<0; \tag{15}$$

$$\frac{d^2E_y^{\mathrm{II}}}{dz^2}-k_0^2(\beta^2-\varepsilon_f)E_y^{\mathrm{II}}+k_0^2\alpha_f(E_y^{\mathrm{II}})^3=0, \quad 0<z<d; \tag{16}$$

$$\frac{d^2E_y^{\mathrm{III}}}{dz^2}-k_0^2(\beta^2-\varepsilon_c)E_y^{\mathrm{III}}=0, \quad z>d. \tag{17}$$

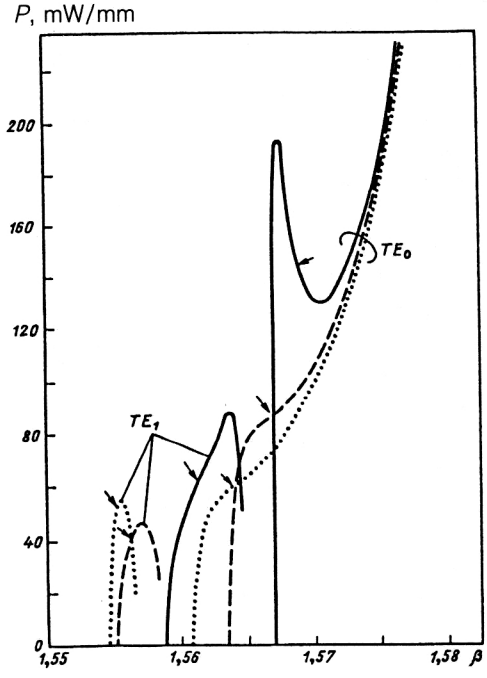

FIG. 2. The same as in Fig. 1 for nonlinear saturable cladding with $\varepsilon_{\mathrm{sat}}=0.1256$. The remaining parameters are the same as in Fig. 1.

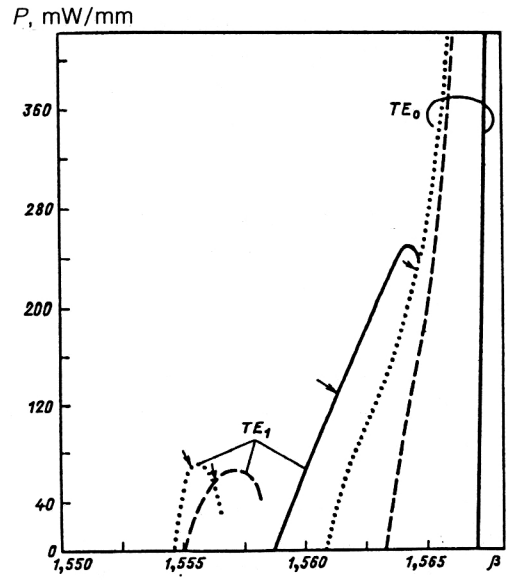

FIG. 3. The same as in Fig. 1 for a nonlinear saturable cladding with $\varepsilon_{\mathrm{sat}}=0.0624$.

We consider solutions localized near the surface of the thin film for which the field tends to zero as $|z|\to\infty$. The exact solutions for $A_0(z)=\alpha_f^{1/2}E_y(z)$ that follow from Eqs. (15)–(17) can be expressed in this case in the form of Jacobi elliptic functions:[62–64]

$$A_0^{\mathrm{I}}(z)=\sqrt{2mt}\,\mathrm{cn}(\varphi/m)\exp(k_0q_cz), \quad z<0; \tag{18}$$

$$A_0^{\mathrm{II}}(z)=\sqrt{2mt}\,\mathrm{cn}(k_0tz+\varphi/m), \quad 0<z<d; \tag{19}$$

$$A_0^{\mathrm{III}}(z)=\sqrt{2mt}\,\mathrm{cn}(u+\varphi/m)\exp[-k_0q_c(z-d)], \quad z>d, \tag{20}$$

where $q_s=(\beta^2-n_s^2)^{1/2}$; $q_c=(\beta^2-n_c^2)^{1/2}$; $t=(|\beta^2-n_f^2|/|2m-1|)^{1/2}$; $u=k_0dt$; m is the parameter of the Jacobi function ($0<m<1$). Here

$$\mathrm{cn}(\varphi/m)=\left[\frac{1}{2m}(2m-1-a^2+r)\right]^{1/2}; \tag{21}$$

$$\mathrm{sn}(\varphi/m)=-\left[\frac{1}{2m}(a^2+1-r)\right]^{1/2}; \tag{22}$$

$$\mathrm{dn}(\varphi/m)=[\tfrac{1}{2}(1-a^2+r)]^{1/2} \tag{23}$$

and $a=-q_s/t$, $r=[(1+a^2)^2-4ma^2]^{1/2}$.

From the boundary conditions, we obtain an eigenvalue equation:

$$\frac{\mathrm{sn}(u+\varphi/m)\mathrm{dn}(u+\varphi/m)}{\mathrm{cn}(u+\varphi/m)}=\frac{q_c}{t}, \tag{24}$$

which is equivalent to an equation of the form

$$\frac{a(\mathrm{dn}^2u-m\,\mathrm{sn}^2\,\mathrm{cn}^2\varphi)+b(\mathrm{dn}^2\varphi-m\,\mathrm{sn}^2\varphi\,\mathrm{cn}^2u)}{(1-ab)(1-m\,\mathrm{sn}^2u\,\mathrm{sn}^2\varphi)}=\frac{q_c}{t}, \tag{25}$$

where $a=-q_s/t=\mathrm{sn}\,\varphi\,\mathrm{dn}\,\varphi/\mathrm{cn}\,\varphi$; $b=\mathrm{sn}\,u\,\mathrm{dn}\,u/\mathrm{cn}\,u$.

The directed energy flux in the wave guide has the form

$$P(\beta)=P_0\beta m t^2\left[\frac{\mathrm{cn}^2(u+\varphi/m)}{q_c}+\frac{\mathrm{cn}^2(\varphi/m)}{q_s}\right]+2P_0\beta t\left[\int_0^u \mathrm{dn}^2(V+\varphi/m)dV-(1-m)k_0 td\right], \quad (26)$$

where $P_0=(2\alpha_f k_0)^{-1}(\varepsilon_0/\mu_0)^{1/2}$. In the approximation of a weakly varying amplitude, we obtain for the dimensionless quantity $A(x,z)=\alpha_f^{1/2}E_y(x,z)$ the equation

$$2i\beta k_0\frac{\partial A}{\partial x}+\frac{\partial^2 A}{\partial z^2}-\gamma^2(z)k_0^2A+\theta(z)k_0^2|A|^2A=0. \quad (27)$$

For $z<0$, we have here $\theta(z)=0$, $\gamma^2(z)=\beta^2-n_s^2$; for $0<z<d$, we have $\theta(z)=1$, $\gamma^2(z)=\beta^2-n_f^2$; for $z>d$, we have $\theta(z)=0$, $\gamma^2(z)=\beta^2-n_c^2$. Note that the x-independent solution of the nonlinear partial differential equation (27), $A(0,z)=A_0(z)$, is determined by the relations (18)–(20) and describes a stationary nonlinear guided wave with effective refractive index β determined by the dispersion relation $\beta=\beta(P)$.

Equation (27) has two integrals of the motion:

$$I(\beta)=k_0\int_{-\infty}^{\infty}|A|^2dz; \quad (28)$$

$$H(\beta)=k_0\int_{-\infty}^{\infty}\left[\left|\frac{1}{k_0}\frac{\partial A}{\partial z}\right|^2+\gamma^2(z)|A|^2-\frac{1}{3}\theta(z)|A|^4\right]dz \quad (29)$$

and for arbitrary solutions we have $dI/dx=dH/dx=0$.

Figure 4 shows the dependence of the effective refractive index β on the dimensionless energy flux P/P_0 for an asymmetric wave guide with nonlinear self-focusing dielectric film of Kerr type.[64] For the chosen wave-guide parameters, the TE_0 and TE_1 guided waves have a threshold behavior (Fig. 4). To avoid laborious calculations, we used the Crank–Nicholson difference scheme[33,64] to solve Eq. (27). The corresponding system of nonlinear equations was solved by the Newton–Picard method. In the considered case, two iterations were sufficient to achieve convergence of this method. This scheme made it possible to conserve the integrals of the motion (28) and (29) on the complete grid.

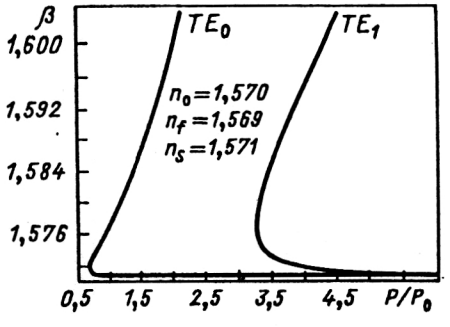

FIG. 4. Dependence of effective refractive index β on the dimensionless energy flux P/P_0 for $n_s=1.571$, $n_f=1.569$, $n_c=1.57$, $d/\lambda=2$, $\lambda=0.633$ μm.

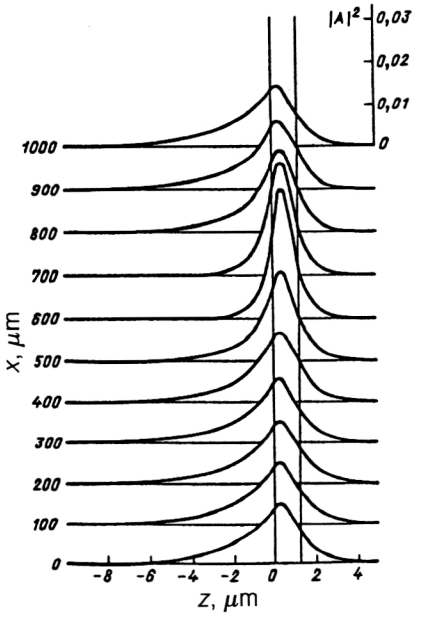

FIG. 5. Evolution of the distribution of TE_0 nonlinear guided wave with propagation distance. The initial distribution corresponds to $\beta=1.5712$. The remaining parameters are as in Fig. 4.

In the absence of dissipation, unstable stationary waves were defined as waves whose field profile with respect to the z coordinate changed after a distance x had been traversed. In other cases, the nonlinear waves were defined as stable. In the absence of loss, the distribution of the optical field remained unchanged for a distance up to 1000 μm traversed along the x axis. Figure 5 shows the results of the numerical solution for the distribution of the stationary field of a TE_0 wave corresponding to a fixed value of β in the region of negative slope of the nonlinear dispersion curve in Fig. 4 and for propagation over a distance up to 1000 μm. The chosen grid dimensions were $k_0\Delta x=3.97$ and $k_0\Delta z=1.26$. The conservation of the integral of the motion $I(\beta)$ after the distance 1000 μm had been traversed along the x axis was good: $I(x=0)=0.776$ and $I(x=1000$ μm$)=0.770$. It is interesting to note that the initial distribution (at $x=0$) of the optical field was almost identical to the field distribution after the distance $x=1000$ μm had been traversed. For the parameters of the calculation shown in Fig. 6, a threshold behavior of β as a function of P/P_0 occurs only for a TE_2 directed wave. The stability of the propagation of the waves corresponding to the branches of the nonlinear dispersion curve with positive slope was checked numerically. Figure 7 shows the numerical result of the process of propagation of the profile of the stationary optical field for the TE_2 wave corresponding to the negative slope of the nonlinear dispersion curve. Here, the grid dimensions were taken to be $k_0\Delta x=3.970$ and $k_0\Delta z=1.985$. For the chosen value of the propagation

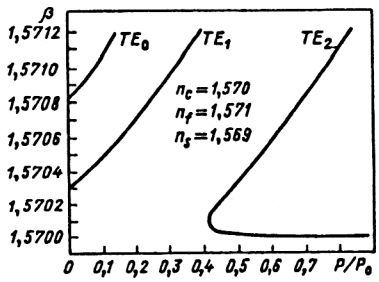

FIG. 6. The same as in Fig. 4 for $n_s = 1.569$, $n_f = 1.571$, $n_c = 1.57$, $d = 10$ μm, $\lambda = 0.633$ μm.

constant, the field varies with x, but the conservation of the integral of the motion $I(\beta)$ after $\Delta x = 6000$ μm is still fairly good: $I(x=0) = 0.490$ and $I(x=6000\ \mu\text{m}) = 0.476$. Thus, the TE_2 branch, corresponding to negative slope of the nonlinear dispersion curve, is unstable.

Effects of absorption of nonlinear optical waves in self-focusing thin films

The effects of linear absorption of nonlinear optical waves in wave guides with linear film dielectric and nonlinear cladding were investigated numerically in Refs. 31 and 32. Below, we consider in detail the effects of linear absorption of a TE_0 nonlinear optical wave propagating in film dielectrics of Kerr type. A characteristic feature of these propagation processes is the tendency of the optical field to avoid a regime that leads to losses, and this results in a certain rearrangement of the properties of the nonlinear guided waves.

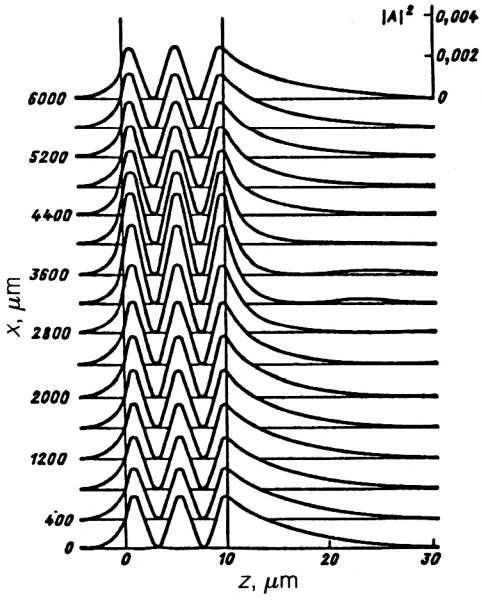

FIG. 7. Evolution of the distribution of TE_2 nonlinear guided wave with propagation distance. The initial distribution corresponds to $\beta = 1.57002$. The remaining parameters are as in Fig. 6.

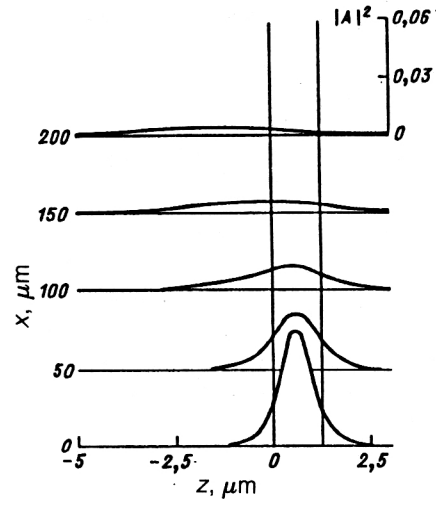

FIG. 8. Evolution of the distribution of TE_0 nonlinear guided wave with propagation distance in the presence of losses ($\Gamma_f = 10^{-3}$, $\Gamma_s = \Gamma_c = 0$). The initial distribution corresponds to $\beta = 1.578$. The remaining parameters are as in Fig. 4.

To take into account absorption, we modify Eq. (27) to the form

$$2i\beta k_0 \frac{\partial A}{\partial x} + \frac{\partial^2 A}{\partial z^2} - \gamma^2(z)k_0^2 A + \theta(z)k_0^2|A|^2 A + i\beta k_0^2 \Gamma(z) A = 0, \tag{30}$$

where $\Gamma(z)$ is the function that characterizes the absorption profile. In the presence of losses, the Kramers–Kronig relation shows that, at the least, nonlinear refraction must be accompanied by linear absorption. For this reason, the linear term $i\beta k_0^2 \Gamma(z) A$ is included in Eq. (30).

To investigate the effects of linear absorption of TE_0 nonlinear optical waves, we solved Eq. (30) with initial conditions corresponding to the exact nonlinear stationary solution, for which the nonlinear dispersion curves are shown in Fig. 4, for $\Gamma_s = \Gamma_c = 0$ and $\Gamma_f \neq 0$; i.e., we restricted ourselves to losses in only the film. For Γ_f we chose a value that is fairly large but realistic for many materials, namely, $\Gamma_f = 10^{-3}$ (Refs. 32 and 36), which corresponds to a characteristic length $L = (k_0 \Gamma_f)^{-1} \cong 100$ μm. In the numerical calculations, the length of the path of propagation of the nonlinear guided waves was taken to be several times greater than the characteristic length.[33] As can be seen from Fig. 8, the clearly expressed maximum in the distribution of the optical field corresponding to a value of β in the region of positive slope of the nonlinear dispersion curve in Fig. 4 is quite strongly flattened after propagation through a distance of the order of the characteristic length L. As a result of the evolution, the self-focusing peak moves in the direction to the substrate, in which there are no losses and in which the refractive index is $n_s > \max(n_f, n_c)$. Figure 9 shows the evolution of the profile of the optical field of the TE_0 wave corresponding to negative slope of the nonlinear dispersion curve. The peak moves from the nonlinear film to the substrate, where the

absorption is weaker and the refractive index is higher. In conclusion, we note that absorption effects become important when one is designing nonlinear optical devices with a length of the order of the characteristic length L.

Nonlinear optical waves guided by self-focusing thin films with nonlinear cladding

We consider nonlinear TE polarized guided waves propagating in a four-layer optical wave guide which consists of a self-focusing dielectric film of Kerr type having on one side a self-focusing cladding of Kerr type and on the other two linear dielectric layers.[65] The nonlinear cladding, which is characterized by the dielectric function $\varepsilon=\varepsilon_c+\alpha_c|\mathbf{E}|^2$, $\alpha_c>0$, is situated in the region $z<0$. The refractive index of the cladding depends on the flux in accordance with the formula $n=n_c+n_{2c}I$ ($n_{2c}>0$). The nonlinear film, which is in the region $0<z<d_1$, has dielectric function of the form $\varepsilon=\varepsilon_{f_1}+\alpha_{f_1}|E|^2$, $\alpha_{f_1}>0$, and, accordingly, refractive index of the form $n=n_{f_1}+n_{2f_1}I$ ($n_{2f_1}>0$). In the region $d_1<z<d_2$ there is a linear dielectric layer characterized by refractive index n_{f_2}, and in the region $z>d_1+d_2$ there is a semi-infinite linear medium characterized by refractive index n_s.

The solution of Maxwell's equation for the dimensionless quantity $A(z)=\alpha_c^{1/2}E_y(z)$ in the regions $z<0$ and $z>d_1+d_2$ has the form

$$A(z)=\sqrt{2}q_c\{\cosh[k_0q_c(z-z_c)]\}^{-1},\quad z<0; \tag{31}$$

$$A(z)=A_{d_1+d_2}\exp[-k_0(z-d_1-d_2)q_s],\quad z>d_1+d_2, \tag{32}$$

where $q_c=(\beta^2-n_c^2)^{1/2}$; $q_s=(\beta^2-n_s^2)^{1/2}$; z_c is an integration constant; $A_{d_1+d_2}$ is the value of $A(z)$ at the boundary $z=d_1+d_2$. The wave equations that determine the nonlinear TE polarized guided waves propagating in the region $0<z<d_1+d_2$ have the form

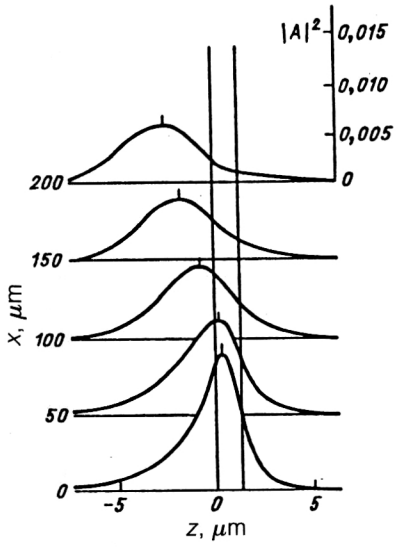

FIG. 9. The same as in Fig. 8 for $\beta=1.5712$.

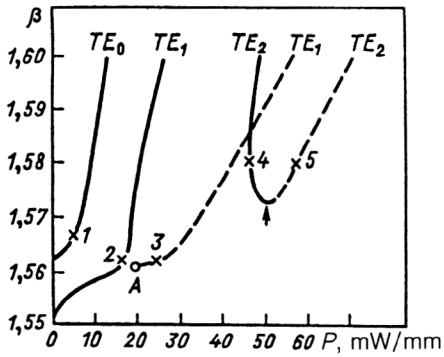

FIG. 10. Dependence of the effective refractive index β on the energy flux P. The parameters of the calculation are: $n_c=1.55$, $n_{2c}=10^{-9}$ m^2/W, $n_{f_1}=1.56$, $n_{2f_1}=3\times10^{-9}$ m^2/W, $n_{f_2}=1.57$, $n_s=1$, $d_1=d_2=2\lambda$, and $\lambda=0.515$ μm.

$$\frac{d^2A}{dz^2}=k_0^2[(\beta^2-n_{f_1}^2)A-rA^3],\quad 0<z<d_1; \tag{33}$$

$$\frac{d^2A}{dz^2}=k_0^2(\beta^2-n_{f_2}^2)A,\quad d_1<z<d_1+d_2, \tag{34}$$

where $r=\alpha_{f_1}/\alpha_c=n_{2f_1}/n_{2c}$. The boundary conditions at the interface $z=0$ lead to the equation

$$\left|\frac{dA}{dz}\right|_{z=0}=-sk_0A_0(\beta^2-n_c^2-\tfrac{1}{2}A_0^2)^{1/2}, \tag{35}$$

where $s=\operatorname{sign}(dA/dz)|_{z=0}$, and A_0 is the value of the dimensionless amplitude at the boundary $z=0$. Thus, for $s=+1$ there exists a maximum of the electric field, which is localized in the nonlinear cladding, while for $s=-1$ there is a maximum localized in the region of the film. Fulfillment of the boundary conditions at the interface $z=d_1+d_2$ leads to the following equation for β:

$$\left|\frac{dA}{dz}\right|_{z=d_1+d_2}+(\beta^2-n_s^2)^{1/2}A_{d_1+d_2}=0. \tag{36}$$

This equation can be solved numerically by means of Newton's method. Determining the value of β, we can calculate the energy flux carried by the guided waves:

$$P(\beta)=P_0\beta[2(\beta^2-n_c^2)^{1/2}+2s(\beta^2-n_c^2-\tfrac{1}{2}A_0^2)^{1/2}+k_0\int_0^{d_1+d_2}[A(z)]^2dz+\tfrac{1}{2}A_{d_1+d_2}^2\times(\beta^2-n_s^2)^{-1/2}], \tag{37}$$

where $P_0=(2\alpha_ck_0)^{-1}(\varepsilon_0/\mu_0)^{1/2}$. The nonlinear equation (33) was solved numerically by means of the Runge–Kutta method in conjunction with the Richardson extrapolation procedure.[65,65] Figure 10 shows the effective refractive index as a function of the energy flux. In the case of the TE_0 wave, there is a linear limit; for the TE_1 wave, two branches arise; one of them has a linear limit; the other has threshold behavior (the termination point A in Fig. 10). In the case of the TE_2 wave, there is also threshold behavior.

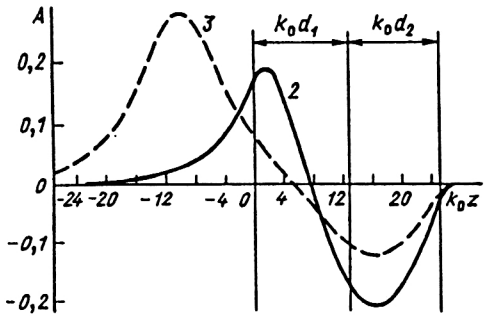

FIG. 11. Dependence of the amplitude A on the dimensionless quantity k_0z for $\beta = 1.562$. The continuous and broken curves correspond to points 2 and 3 on the nonlinear dispersion curve in Fig. 10.

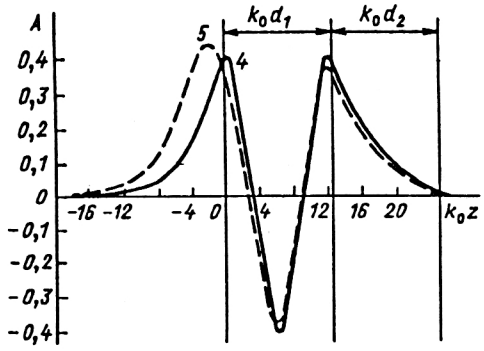

FIG. 12. The same as in Fig. 11 for $\beta = 1.58$. The continuous and broken curves correspond to the points 4 and 5 on the nonlinear dispersion curve in Fig. 10.

The continuous curves correspond to the position of the field maximum in the region $0 < z < d_1 + d_2$, and the broken curves correspond to the maximum of the optical field, which is situated near the interface between the nonlinear cladding and the nonlinear film and tends to the region of the nonlinear self-focusing cladding when the energy flux is increased. The arrow in Fig. 10 indicates the transition point, when the field maximum is localized at the interface of the nonlinear cladding and the nonlinear film. Point 1 in the nonlinear dispersion curve corresponds to a maximum of the optical field localized in the film near the interface between the nonlinear dielectric film of thickness d_1 and the linear dielectric film of thickness d_2. Figure 11 shows the dimensionless amplitude A as a function of the dimensionless coordinate k_0z for the TE_1 wave for two points 2 and 3, which correspond to the same value of β. As can be seen from Fig. 11, one of the maxima of the TE_1 branch, corresponding to point 3, is localized in the nonlinear self-focusing cladding layer, whereas the other is concentrated in the thin linear film of thickness d_2. Figure 12 shows the distribution of the field for the TE_2 wave for points 4 and 5 of the nonlinear dispersion curve corresponding to the given value of β. For point 5, one of the three maxima of the TE_2 wave is situated near the boundary of the nonlinear cladding, to which it tends with increasing energy flux.

Figure 13 shows the nonlinear dispersion curves for a different set of parameters. For the TE_0 wave there are two disconnected branches, one of which has a linear limit, while the other has threshold behavior. The continuous curves correspond to the case $s = -1$ [see Eq. (37)], when the maximum of the optical field is localized in the film. The broken curves correspond to the case $s = +1$, when the maximum is in the nonlinear cladding (the arrows indicate the transition points). For the TE_1 wave there is also self-focusing in the cladding, and in this case the corresponding nonlinear dispersion curve has a termination point (point A in Fig. 13). The propagation of the TE_1 wave is characterized by the presence of an absolute value of the maximum of the guided energy flux. Points 1 and 2 of the nonlinear dispersion curve for the TE_0 wave correspond to localization of the maximum in the nonlinear self-focusing film of thickness d_1. Point 3 corresponds to localization of the maximum of the optical field in the nonlinear cladding layer. With increasing effective refractive index β, the maximum of the low-power TE_1 wave, which is situated in the nonlinear dielectric film near the nonlinear cladding layer, moves toward the boundary medium (points 4 and 5 of the nonlinear dispersion curve in Fig. 13).

3. EMISSION OF SOLITONS FROM NONLINEAR PLANAR OPTICAL WAVE GUIDES

The problem of multisoliton emission from nonlinear optical wave guides in which there are no losses and there is a Kerr-type or saturable cladding was investigated numerically by the beam-propagation method in Refs. 35 and 37. This method was also used in Ref. 67 to study the effects of nonlinear absorption of TE_m nonlinear guided waves. The effect of absorption and saturation on soliton emission in nonlinear planar optical wave guides was analyzed in Refs. 36 and 68.

The equation on which the analysis is based is a linear–nonlinear equation of Schrödinger type. For the solution of the parabolic differential equation, an algorithm that has become known as the beam-propagation method is quite widely employed at the present time. However, it requires much computing time. Besides this algorithm, the Crank–Nicholson method is used in conjunction with the

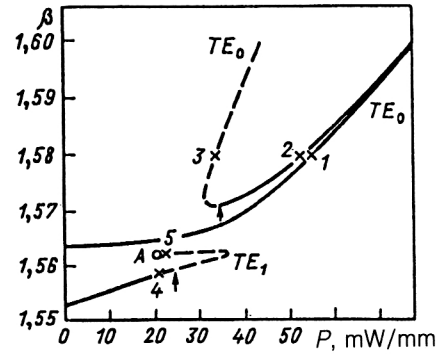

FIG. 13. The same as in Fig. 10. The parameters of the calculation are $n_c = 1.55$, $n_{2c} = 10^{-9}$ m^2/W, $n_{f_1} = 1.56$, $n_{2f_1} = 0.5 \times 10^{-9}$ m^2/W, $n_{f_2} = 1.57$, $n_s = 1.52$, $d_1 = d_2 = 2\lambda$, and $\lambda = 0.515$ μm.

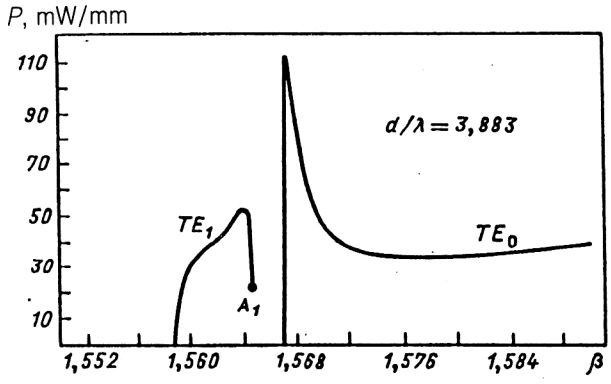

FIG. 14. Nonlinear dispersion curve $P=P(\beta)$ for TE_m nonlinear guided waves. The parameters of the calculation are $n_s=1.55$, $n_f=1.57$, $n_c=1.55$, $n_{2c}=10^{-9}$ m^{2}W, $d=2$ μm, $\lambda=0.515$ μm.

Newton–Picard iterative procedure to solve Eq. (30).[33,69,70] In this case, the computing time is significantly shortened.

Thin-film optical wave guides with nonlinear cladding of Kerr type

We consider a three-layer planar wave guide consisting of an optically linear substrate characterized by dielectric constant $\varepsilon_s=n_s^2$ in the region $z<0$, a thin dielectric film of thickness d characterized by refractive index $n_f^2=\varepsilon_f$ in the region $0<z<d$, and a nonlinear self-focusing cladding of Kerr type characterized by dielectric tensor $\varepsilon_{xx}=\varepsilon_{yy}=\varepsilon_{zz}=\varepsilon_c+\alpha_c|\mathbf{E}|^2$ $(\alpha_c>0)$ in the region $z<d$. Solving Maxwell's equations and using the approximation of a slowly varying amplitude, we arrive at an equation of the form (27), in which

$$\theta(z)=\begin{cases}1, & -\infty<z<d;\\ 0, & z<d.\end{cases}$$

The x-independent solution of Eq. (27), $A(0,z)=A_0(z)$, is a stationary nonlinear guided wave with effective refractive index β determined by means of the nonlinear dispersion curve (Fig. 14). The corresponding grid dimensions used in the finite-difference scheme were taken to be $k_0\Delta x=k_0\Delta z=0.4$ We made a numerical experiment in which we fixed the field profile of the input beam propagating in the nonlinear wave guide and varied the energy flux. As input beam, we chose a linear TE_0 mode, for which the value of the linear effective refractive index β_0 was determined as the largest value satisfying the linear dispersion relation

$$\tan(k_0q_fd)=\frac{q_f(q_s+q_c)}{(q_f^2-q_sq_c)}, \tag{38}$$

where

$$q_s=(\beta^2-n_s^2)^{1/2},\quad q_f=(n_f^2-\beta^2)^{1/2},\quad q_c=(\beta^2-n_c^2)^{1/2}.$$

The dimensionless amplitude $A_0(z)$ of the input beam was determined as follows:[4]

$$A_0(z)=A_s\exp(k_0q_sz),\quad z<0; \tag{39}$$

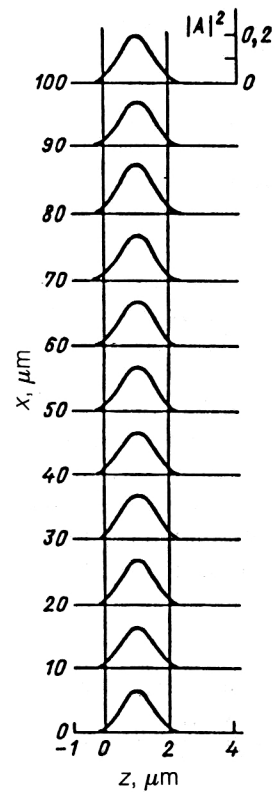

FIG. 15. Evolution of the linear TE_0 field in the absence of losses for $P=75$ mW/mm.

$$A_0(z)=A_f\cos(k_0q_fz-\Phi_{sf}),\quad 0<z<d; \tag{40}$$

$$A_0(z)=A_c\exp[-k_0q_c(z-d)],\quad z>d, \tag{41}$$

where $\Phi_{sf}=\tan^{-1}(q_s/q_f)$;

$$A_s=A_f\left(\frac{n_f^2-\beta^2}{n_f^2-n_s^2}\right)^{1/2};\quad A_c=A_f\left(\frac{n_f^2-\beta^2}{n_f^2-n_c^2}\right)^{1/2}; \tag{42}$$

and the amplitude A_f is related to the total energy flux transmitted in the wave guide by

$$A_f=\left(\frac{2P}{k_0d_{\text{eff}}\beta P_0}\right)^{1/2}. \tag{43}$$

Here, $d_{\text{eff}}=d+(k_0q_c)^{-1}+(k_0q_s)^{-1}$ is the effective thickness of the wave-guide film, and $P_0=(2\alpha_ck_0)^{-1}(\varepsilon_0/\mu_0)^{1/2}$. For the values $\beta=\beta_0$ and $P=75$ mW/mm, the profile of the input beam (TE_0 linear mode) agrees closely with the profile of the nonlinear wave-guide TE wave (Fig. 15). For $P=112$ mW/mm, part of the initial energy flux goes into the self-focusing channel; i.e., there is emission of a spatial soliton through the film–cladding interface with the nonlinear self-focusing cladding (Fig. 16).

Effect of absorption on soliton emission

As we have already noted, in the presence of dissipation it is necessary to take into account absorption terms, which in the simplest case are proportional to the amplitude $i\beta k_0^2\Gamma(z)A$ [see Eq. (30)]. We consider the effect of

absorption in the case of emission of a single soliton from a nonlinear planar optical wave guide with self-focusing cladding of Kerr type. Suppose $\Gamma_s=\Gamma_f=0$, $\Gamma_c=10^{-3}$ and the input energy flux is $P=112$ mW/mm, when there is separation of the single soliton in the absence of loss. It can be seen from Fig. 17 that although there is emission of a localized wave packet, there is a significant decrease of the transmitted energy along the wave guide, and also a significant broadening of the profile of the transmitted flux of the soliton-like wave as the propagation takes place. In addition, with the decrease in the energy carried by the optical wave there is a loss of velocity of the wave packet moving from the film–cladding interface compared with the velocity of soliton emission in the absence of dissipation. With increasing loss in the cladding (Fig. 18), soliton emission into the nonlinear cladding ceases, and the profile of the optical field is similar to the profile of an ordinary linear TE_0 wave, although the amplitude decreases with the propagation in the wave guide.

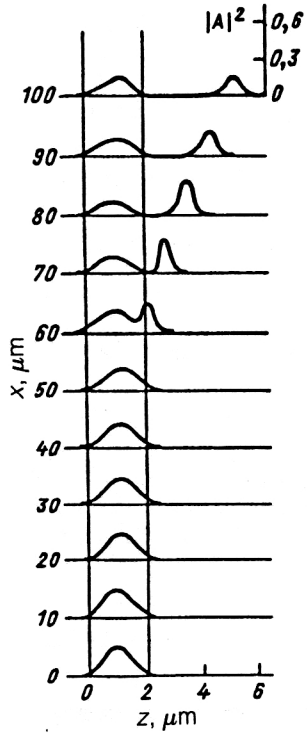

FIG. 17. Soliton emission in the presence of absorption for $P=112$ mW/mm for $\Gamma_s=\Gamma_f=0$ and $\Gamma_c=10^{-3}$.

4. NONLINEAR SURFACE AND GUIDED WAVES IN PERIODIC DIELECTRIC STRUCTURES OF STEP PROFILE. THE TRANSFER-MATRIX METHOD

Nonlinear surface waves propagating in semi-infinite periodic dielectrics with step profile and contiguous with Kerr-type media

We consider a system that consists of a nonlinear material in the region $z<0$ characterized by dielectric constant $\varepsilon=\varepsilon_c+\alpha_c|\mathbf{E}|^2$ $(\alpha_c>0)$ and a multilayer material in the region $z>0$ containing layers A and B of thicknesses d_1

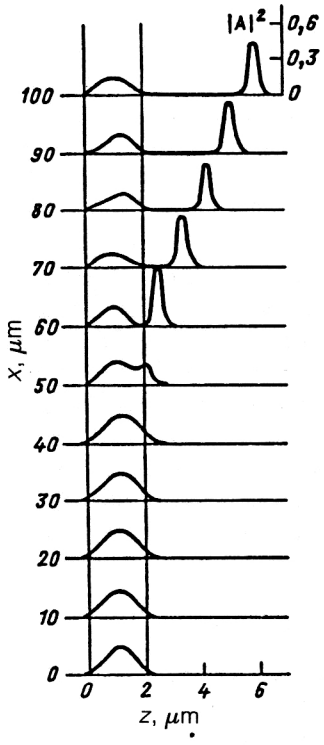

FIG. 16. The same as in Fig. 15 for $P=112$ mW/mm.

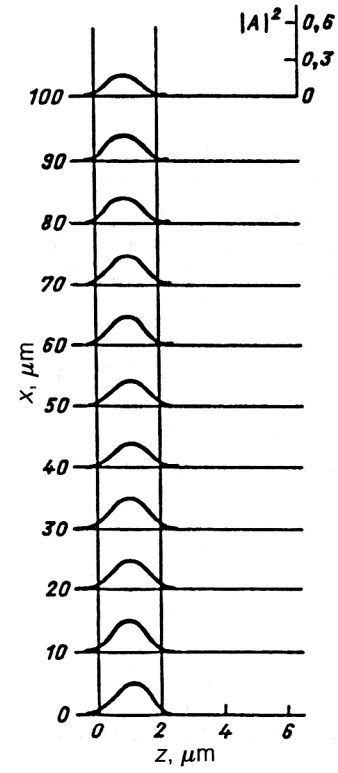

FIG. 18. The same as in Fig. 17 for $\Gamma_s=\Gamma_f=0$ and $\Gamma_c=10^{-2}$.

and d_2 and characterized by the refractive indices n_1 and n_2, respectively.

The exact solution of Maxwell's equations in the case of a nonlinear cladding of Kerr type is determined by the relation (7), where $q_c=(\beta^2-\varepsilon_c)^{1/2}$, and z_c is an integration constant. We introduce the dimensionless parameter u:

$$u=\frac{1}{k_0 q_c}\left[\frac{d}{dz}\ln E_y\right]_{z=0}. \tag{44}$$

From the relations (7) and (44) we find that $E_0=(2/\alpha_c)^{1/2}q_c(1-u^2)^{1/2}$, where $-1\leqslant u\leqslant 1$, and E_0 is the value of the electric field at the nonlinear interface $z=0$.

The general solution of Maxwell's equations in the case of a periodic dielectric structure of step profile with boundary conditions at $z=(n+1)d$, $n=0,1,2,...$, can be written in the form

$$E_y(z)=A_n^c\cosh[k_0q_1(z-nd)]+\frac{A_n^s}{q_1}\sinh[k_0q_1(z-nd)] \tag{45}$$

for $nd\leqslant z\leqslant nd+d_1$ and

$$E_y(z)=A_{n+1}^c\cosh[k_0q_2(z-d(n+1))]+\frac{A_{n+1}^s}{q_2}\sinh[k_0q_2(z-d(n+1))] \tag{46}$$

for $nd+d_1\leqslant z\leqslant(n+1)d$. Here $n=0,1,2,...,d=d_1+d_2$, $q_{1,2}=(\beta^2-\varepsilon_{1,2})^{1/2}$, $\varepsilon_{1,2}=n_{1,2}^2$, $A_0^c=E_0$, and $A_0^s=uq_cE_0$.

The boundary conditions at $z=nd+d_1$ lead to the following relation between the coefficients $A_{n+1}^{c,s}$ and $A_n^{c,s}$:

$$\begin{pmatrix}A_{n+1}^c\\A_{n+1}^s\end{pmatrix}=T\begin{pmatrix}A_n^c\\A_n^s\end{pmatrix},\quad n=0,1,2..., \tag{47}$$

where the transfer matrix T is determined by

$$T=\begin{pmatrix}\cosh\gamma_1\cosh\gamma_2+\dfrac{q_1}{q_2}\sinh\gamma_1\sinh\gamma_2 & \dfrac{1}{q_2}\cosh\gamma_1\sinh\gamma_2+\dfrac{1}{q_1}\sinh\gamma_1\cosh\gamma_2\\ q_2\cosh\gamma_1\sinh\gamma_2+q_1\cosh\gamma_2 & \cosh\gamma_1\cosh\gamma_2+\dfrac{q_2}{q_1}\sinh\gamma_1\sinh\gamma_2\end{pmatrix}. \tag{48}$$

The eigenvalues $\lambda_\pm$ of the transfer matrix have the form

$$\lambda_\pm=s\exp(\pm tk_0d)=[\,|f(\beta)|\pm\Delta^{1/2}]\operatorname{sign}[f(\beta)], \tag{49}$$

where $t>0$ for real values and $\operatorname{Im}t>0$ in the case of imaginary values. In addition,

$$\left.\begin{aligned}&s=\operatorname{sign}[f(\beta)];\\&f(\beta)=\cosh\gamma_1\cosh\gamma_2+\frac{1}{2}\left(\frac{q_1}{q_2}+\frac{q_2}{q_1}\right)\sinh\gamma_1\sinh\gamma_2;\\&\Delta=[f(\beta)]^2-1.\end{aligned}\right\} \tag{50}$$

The eigenvectors $V_\pm$ corresponding to the eigenvalues $\lambda_\pm$ are determined by expressions of the form

$$V_\pm=\begin{pmatrix}1\\a_\pm\end{pmatrix}; \tag{51}$$

$$a_\pm=\frac{\left[\frac{1}{2}\left(\frac{q_2}{q_1}-\frac{q_1}{q_2}\right)\sinh\gamma_1\sinh\gamma_2\pm s\Delta^{1/2}\right]}{\left(\frac{\sinh\gamma_1}{q_1}\cosh\gamma_2+\frac{\sinh\gamma_2}{q_2}\cosh\gamma_1\right)}. \tag{52}$$

In accordance with the expression (47), we have

$$\begin{pmatrix}A_n^c\\A_n^s\end{pmatrix}=T^n\begin{pmatrix}A_0^c\\A_0^s\end{pmatrix},\quad n=0,1,2,... \tag{53}$$

When $\Delta\neq 0$, we have $a_+\neq a_1$, and the quantities $A_0^{c,s}$ can be expressed by means of the linearly independent vectors $V_\pm$:

$$A^\pm=(a_\mp-uq_c)(a_+-a_-)^{-1}, \tag{54}$$

where $A^\pm=(a_\mp-uq_c)(a_+-a_-)^{-1}$. Substituting the expression (54) in the relation (53), we obtain

$$\begin{pmatrix}A_n^c\\A_n^s\end{pmatrix}=s^n[A^-\exp(-ntk_0d)V_--A^+\exp(ntk_0d)V_+]. \tag{55}$$

A nonlinear surface wave exists if there is an exponential decrease of the field at a large distance from the interface between the two semi-infinite media, i.e., $A^+=0$ and $a_-=uq_c$. Moreover, t must be real and $\Delta\geqslant 0$ [see the relation (49)]. Note that for $u=1$ we obtain the dispersion relation $a_-(\beta)-q_c(\beta)=0$ for a linear surface wave propagating along the interface between linear dielectric media when one of them has a periodic structure of step profile.

The energy flux of the guided surface waves is determined by the Poynting vector

$$P/P_{0c}=2\beta q_c(1-u)+\beta q_c^2(1-u^2)[1-\exp(-2tk_0d)]^{-1}\times[F_1^++\exp(-2tk_0d)F_2^-], \tag{56}$$

where

$$P_{0c}=(2\alpha_ck_0)^{-1}(\varepsilon_0/\mu_0)^{1/2}$$

and

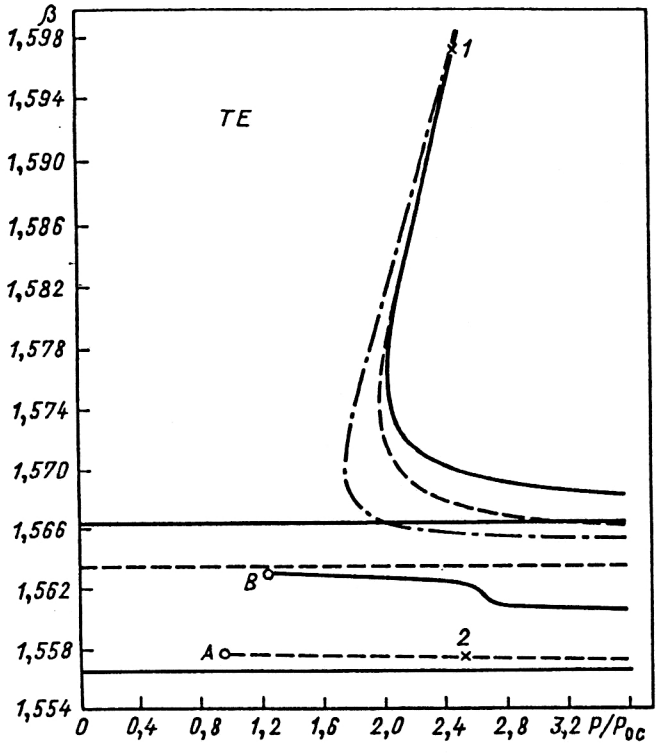

FIG. 19. Dependence of the effective refractive index β on the dimensionless flux P/P_{0c}. The parameters of the calculation are $n_c = 1.55$, $n_1 = 1.57$, $n_2 = 1.56$, $d_1 = d_2 = \delta\lambda$. The chain curve is for $\delta = 0.05$, the broken curves for $\delta = 2$, and the continuous curves for $\delta = 3$.

$$F_{1,2}^{\pm} = \frac{\sinh\gamma_{1,2}\cosh\gamma_{1,2} + \gamma_{1,2}}{q_{1,2}} \pm 2uq_c\left(\frac{\sinh\gamma_{1,2}}{q_{1,2}}\right)^2 + u^2q_c^2\frac{\sinh\gamma_{1,2}\cosh\gamma_{1,2} - \gamma_{1,2}}{q_{1,2}^3}. \quad (57)$$

Figure 19 shows the nonlinear dispersion curves for different values of the thickness parameter of the layers, for which $d_1 = d_2 = \delta\lambda$. For $\delta \ll 1$, the properties of the periodic multilayer structure are similar to those of a homogeneous material characterized by dielectric constant

$$\tilde{\varepsilon} = \frac{d_1\varepsilon_1 + d_2\varepsilon_2}{d_1 + d_2}.$$

In this case, $\beta > \beta_0 \cong \tilde{\varepsilon}^{1/2}$, where β_0 is determined from the equation $f(\beta_0) = 1$. In the case $\delta = 0.05$ (chain curves in Fig. 19), the result for the nonlinear dispersion curve obtained from the dispersion relation $\beta = \beta(P)$ is similar to the result for the curve for a *TE* nonlinear surface wave propagating at the interface between a nonlinear medium of Kerr type and a linear cladding.[4,5] for $\beta > \max(n_1, n_2)$, both quantities q_1 and q_2 are real; accordingly, $f(\beta) > 1$, and we have $s = +1$, $\Delta > 0$, and $-1 < u < 1$. At the same time, the corresponding nonlinear dispersion curve is a continuous function of β. For $\beta < \max(n_1, n_2)$, the conditions for the existence of a nonlinear surface wave ($\Delta \geqslant 0$, $-1 \leqslant u \leqslant 1$) are realized only for certain values of β. Moreover, a "strip structure" arises for the nonlinear dispersion

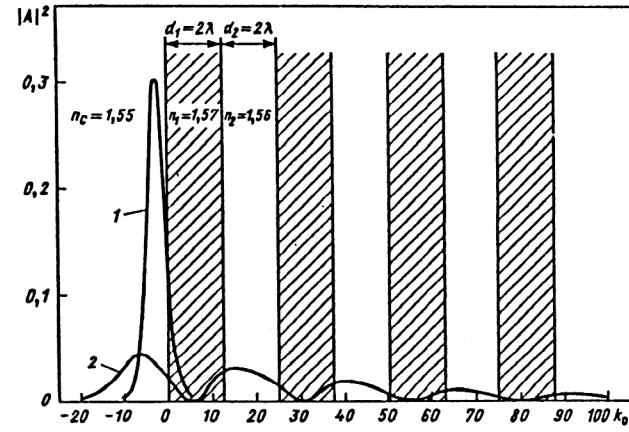

FIG. 20. Dependence of the square $|A|^2$ of the field amplitude on the dimensionless quantity k_0z for $\beta = 1.597$ (point 1 on the nonlinear dispersion curve in Fig. 19) and for $\beta = 1.5573$ (point 2 on the same curve).

curve when definite values of δ are chosen. The "strip edges" correspond to the conditions $\Delta = 0$ ($P/P_{0c} \to \infty$), $u = 1$ ($P/P_{0c} = 0$), and $u = -1$.

In the case $\delta = 2$ (broken curves in Fig. 19), we have three branches of nonlinear dispersion curves, which are separated because of the forbidden values of β. The termination point A of the lowest branch corresponds to the value $u = -1$. With increasing thickness $d = d_1 + d_2$ of an individual cell of the periodic dielectric structure with step profile, the number of branches of the nonlinear dispersion curve increases. For example, for $\delta = 3$ (continuous curves in Fig. 19), there are four different branches. Two of them have a linear limit, to which the largest value $u = 1$ corresponds. This termination point B in Fig. 19 corresponds to the smallest allowed value: $u = -1$.

Figure 20 shows the square of the dimensionless amplitude $|A|^2 = \alpha_c[E_y(z)]^2$ as a function of the dimensionless coordinate k_0z for $\delta = 2$ and two values of the effective refractive index $\beta_1 = 1.597$, $\beta_2 = 1.5573$, which correspond to the same value of the relative energy flux: $P/P_{0c} \cong 2.5$. For β_1 in the region of positive slope of the upper nonlinear dispersion curve (point 1 in Fig. 19), there exists only one maximum of the optical field, which is concentrated at the interface between the nonlinear self-focusing substrate and the linear periodic structure of step profile. For β_2 on the lower branch of the nonlinear dispersion curve (point 2 in Fig. 19), one of the field maxima is localized in the nonlinear substrate, and the others are localized in the linear structure. The field itself is mainly concentrated in the region of the periodic linear structure.

Figure 21 shows examples of the nonlinear dispersion curves for other sets of parameters when $n_1 < n_2$. For $\delta = 2$ (broken curves) there are two branches of nonlinear dispersion curves, each of which is characterized by threshold values of the energy flux. For $\delta = 3$ (continuous curves), there are three different branches separated by forbidden intervals of the values of β. Two of them have threshold values, while the lowest branch has a linear limit.

We consider a multilayer dielectric in which the region

$z<0$ is occupied by a nonlinear self-focusing material of Kerr type (cladding) characterized by dielectric tensor of the form

$$\left.\begin{aligned}\varepsilon_{xx}&=\varepsilon_c+\alpha_c(|E_x|^2+\gamma|E_z|^2);\\ \varepsilon_{zz}&=\varepsilon_c+\alpha_c(\gamma|E_x|^2+\gamma|E_z|^2).\end{aligned}\right\} \tag{58}$$

Here $\alpha_c>0$. The quantity γ models the electron nonlinearity, the molecular orientation, and the nonlinearities which arise due to heating. We take the values of this quantity equal to 1/3, $-1/2$, and 1, respectively. The region $z>0$ is occupied by a semi-infinite periodic medium of step profile containing two alternating layers 1 and 2 of thicknesses d_1 and d_2 and refractive indices n_1 and n_2, respectively. Suppose that a *TM* wave propagates along the x axis. The corresponding magnetic field has the form

$$\mathbf{H}=\tfrac{1}{2}\mathbf{j}H_y(z)\exp[i(\beta k_0 x-\omega t)]+\text{c.c.} \tag{59}$$

Maxwell's equations are written in the form

$$\frac{dH_y}{dz}=ik_0\varepsilon_0 c\varepsilon_{xx}E_x; \tag{60}$$

$$\frac{dE_x}{dz}=i\beta k_0 E_z+ik_0\mu_0 cH_y; \tag{61}$$

$$\beta H_y+\varepsilon_0 c\varepsilon_{zz}E_z=0. \tag{62}$$

The general solution of Maxwell's equations for a linear medium of the type of a superlattice satisfying boundary conditions at $z=nd$ $(d=d_1+d_2)$ has the form

$$H_y(z)=A_n^c\cosh[k_0q_1(z-nd)]A_n^s\frac{\varepsilon_1}{q_1}\sinh[k_0q_1(z-nd)] \tag{63}$$

for $nd\leqslant z\leqslant nd+d_1$ and

$$H_y(z)=A_{n+1}^c\cosh[k_0q_2(z-d(n+1))]+A_{n+1}^s\frac{\varepsilon_2}{q_2}\sinh[k_0q_2(z-d(n+1))] \tag{64}$$

for $nd+d_1\leqslant z\leqslant(n+1)d$. Here, the "unit cell" is identified by the index $n=0,1,2,...$, and $q_{1,2}=(\beta^2-\varepsilon_{1,2})^{1/2}$.

We introduce the parameter u:

$$u=\frac{\varepsilon_c}{k_0q_c}\left[\frac{1}{\varepsilon_{xx}}\frac{d}{dz}\ln H_y\right]_{z=0} \tag{65}$$

and $\beta_c=(\beta^2-\varepsilon_c)^{1/2}$. For a linear dielectric (cladding), we have $u=1$, and from the boundary conditions at $z=0$ we obtain $A_0^c=H_0$ and $A_0^s=\varepsilon_c^{-1}q_cuH_0$, where $H_0=H_y(0)$. Fulfillment of the boundary conditions at $nd+d_1$ leads to the following recursion relation for $A_n^{c,s}$:

$$\begin{pmatrix}A_n^c\\A_n^s\end{pmatrix}=(T_2T_1)^n\begin{pmatrix}A_0^c\\A_0^s\end{pmatrix},\quad n=0,1,2,..., \tag{66}$$

where $T=T_2T_1$ is the transfer matrix with

$$T_{1,2}=\begin{pmatrix}\cosh\gamma_{1,2} & \varepsilon_{1,2}q_{1,2}^{-1}\sinh\gamma_{1,2}\\ \varepsilon_{1,2}^{-1}q_{1,2}\sinh\gamma_{1,2} & \cosh\gamma_{1,2}\end{pmatrix} \tag{67}$$

and $\gamma_{1,2}=k_0q_{1,2}d_{1,2}$. Therefore, we have

$$\begin{pmatrix}A_n^c\\A_n^s\end{pmatrix}=H_0T^n\begin{pmatrix}1\\\varepsilon_c^{-1}q_cu\end{pmatrix}. \tag{68}$$

The relation (68) simplifies appreciably if the vector

$$\begin{pmatrix}1\\\varepsilon_c^{-1}q_c^u\end{pmatrix}$$

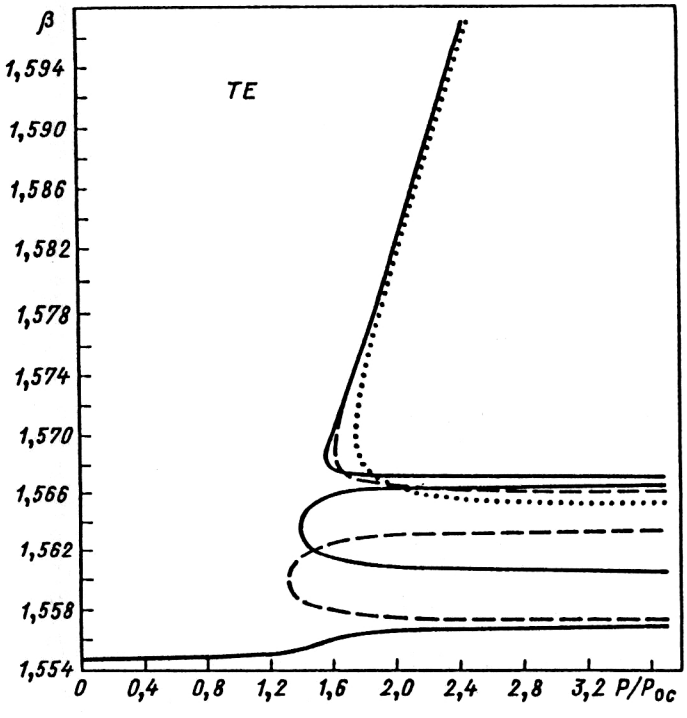

FIG. 21. The same as in Fig. 19. The parameters of the calculation are $n_c=1.55$, $n_1=1.56$, $n_2=1.57$, $d_1=d_2=\delta\lambda$. The broken curves are for $\delta=2$, the dotted curve is for $\delta=0.05$, and the continuous curves are for $\delta=3$.

is represented as a combination of the eigenvectors of the transfer matrix T. The eigenvectors of the transfer matrix, i.e.,

$$TV_{\pm}=s\exp(\pm tk_0d)V_{\pm},$$

have the form

$$V_{\pm}=\begin{pmatrix}1\\ b_{\pm}\end{pmatrix}, \tag{69}$$

where

$$b_{\pm}=\frac{\frac{1}{2}\left(\frac{\varepsilon_1}{\varepsilon_2}\frac{q_2}{q_1}-\frac{\varepsilon_2}{\varepsilon_1}\frac{q_1}{q_2}\right)\sinh\gamma_1\sinh\gamma_2\pm s\Delta^{1/2}}{\left(\frac{\varepsilon_1}{q_1}\sinh\gamma_1\cosh\gamma_2+\frac{\varepsilon_2}{q_2}\sinh\gamma_2\cosh\gamma_1\right)}; \tag{70}$$

$$\exp(\pm tk_0d)=|f(\beta)|\pm\Delta^{1/2}; \tag{71}$$

$$f(\beta)=\cosh\gamma_1\cosh\gamma_2+\frac{1}{2}\left(\frac{\varepsilon_1q_2}{\varepsilon_2q_1}+\frac{\varepsilon_2q_1}{\varepsilon_1q_2}\right)\sinh\gamma_1\sinh\gamma_2. \tag{72}$$

Here, $s=\operatorname{sign}[f(\beta)]$ and $\Delta=[f(\beta)]^2-1$. If $\Delta\neq0$, then $V_+\neq V_-$ and, accordingly,

$$\begin{pmatrix}1\\ \varepsilon_c^{-1}q_cu\end{pmatrix}=A^-V_--A^+v_+, \tag{73}$$

where $A^{\pm}=(b_+-b_-)^{-1}(b_{\mp}-\varepsilon_c^{-1}q_cu)$.

The magnetic field must decrease exponentially with distance, so that $A^+=0$ and $A^-=1$, i.e., $u=\varepsilon_cq_c^{-1}b_-$ and

$$\begin{pmatrix}A_n^c\\ A_n^s\end{pmatrix}=H_0s^n\exp(-ntk_0d)\begin{pmatrix}1\\ \varepsilon_c^{-1}q_cu\end{pmatrix}. \tag{74}$$

The total energy flux is defined as $P=P_{NL}+P_{SL}$, where P_{NL} and P_{SL} are the energy fluxes in the nonlinear substrate and in the semi-infinite superlattice, respectively. The expression for the energy flux in the semi-infinite periodic structure of step profile has the form

$$P_{SL}=P_0\beta g[1-\exp(-2tk_0d)]^{-1}\times[F_1+\exp(-2tk_0d)F_2]. \tag{75}$$

Here

$$F_i=\frac{\cosh\gamma_i\sinh\gamma_i+\gamma_i}{\varepsilon_iq_i}+(-1)^{i+1}2b_-\left(\frac{\sinh\gamma_i}{q_i}\right)^2+\varepsilon_ib_-^2\frac{\cosh\gamma_i\sinh\gamma_i-\gamma_i}{q_i^3}\quad(i=1,2); \tag{76}$$

$$g=\frac{\varepsilon_{z0}^2[(\varepsilon_{z0}-\varepsilon_c)-(\varepsilon_{x0}-\varepsilon_c)]}{2}[\beta^2(1-\gamma^2)]^{-1}, \tag{77}$$

where $\varepsilon_{x0}=\varepsilon_{xx}|_{z=0}$ and $\varepsilon_{z0}=\varepsilon_{zz}|_{z=0}$.

We calculate the energy flux P_{NL} in the nonlinear substrate. A first integral of Maxwell's equations is

$$\alpha\frac{\mu_0}{\varepsilon_0}H_y^2=\frac{\varepsilon_{zz}^2[\varepsilon_{zz}^2[\varepsilon_{zz}-\gamma\varepsilon_{xx}-(1-\gamma)\varepsilon_c]}{\beta^2(1-\gamma^2)}=\frac{\varepsilon_{zz}[\varepsilon_{xx}^2+\varepsilon_{zz}^2-2\varepsilon_c^2-2\gamma(\varepsilon_{xx}\varepsilon_{zz}-\varepsilon_c^2)]}{(2\beta^2-\varepsilon_{zz})(1-\gamma^2)}. \tag{78}$$

By means of it, we can find ε_{xx} as a function of ε_{zz}:

$$\varepsilon_{xx}=\beta^{-2}[(B^2+\beta^2A)^{1/2}-B]. \tag{79}$$

Here

$$A=2\gamma\varepsilon_c[\beta^2(\varepsilon_{zz}-\varepsilon_c)+\varepsilon_{zz}(\beta^2-\varepsilon_{zz})]+(\varepsilon_{zz}-\varepsilon_c)\times[2\varepsilon_{zz}(\beta^2-\varepsilon_{zz})+\beta^2(\varepsilon_{zz}-\varepsilon_c)]+\beta^2\varepsilon_c^2; \tag{80}$$

$$B=\gamma\varepsilon_{zz}(\beta^2-\varepsilon_{zz}). \tag{81}$$

We determine the coordinate z by means of the dielectric constant ε_{zz}. Bearing in mind that

$$\left(\frac{d\varepsilon_{zz}}{dz}\right)^2=k_0^2F(\varepsilon_{zz}), \tag{82}$$

where

$$F(\varepsilon_{zz})=4\beta^2\varepsilon_{xx}^2\frac{\varepsilon_{xx}-\gamma\varepsilon_{zz}-(1-\gamma)\varepsilon_c][\varepsilon_{zz}-\gamma_{xx}-(1-\gamma)\varepsilon_c}{2(\varepsilon_{zz}-\varepsilon_c)-2\gamma(\varepsilon_{xx}-\varepsilon_c)+\varepsilon_{zz}\left(1-\gamma\frac{d\varepsilon_{xx}}{d\varepsilon_{zz}}\right)}; \tag{83}$$

$$\frac{d\varepsilon_{xx}}{d\varepsilon_{zz}}=\beta^{-2}(B^2+\beta^2A)^{-1/2}(\beta^2-\varepsilon_{zz})\{\gamma^2(\beta^2-2\varepsilon_{zz})\varepsilon_{zz}+\beta^2[3\varepsilon_{zz}-2(1-\gamma)\varepsilon_c]\}-\beta^{-2}\gamma(\beta^2-2\varepsilon_{zz}), \tag{84}$$

we finally find

$$z=k_0^{-1}\int_{\varepsilon_{z0}}^{\varepsilon_{zz}}\left[\operatorname{sign}\left(\frac{d\varepsilon'_{zz}}{dz}\right)\right][F(\varepsilon'_{zz})]^{-1/2}d\varepsilon'_{zz}. \tag{85}$$

The component ε_{z0} can be determined from the boundary conditions at $z=0$:

$$(\beta^2-\varepsilon_c)^2u^4\varepsilon_{z0}^5-\varepsilon_cu^2(\beta^2-\varepsilon_c)[u^2(\beta^2-\varepsilon_c)(1-2\gamma)-2\gamma\varepsilon_c]\varepsilon_{z0}^4-2\beta^2\varepsilon_c^2u^2(\beta^2-\varepsilon_c)\varepsilon_{z0}^3+2\beta^2\varepsilon_c^3[u^2\times(\beta^2-\varepsilon_c)+\varepsilon_c]\varepsilon_{z0}^2-3\beta^4\varepsilon_c^4\varepsilon_{z0}+\beta^4\varepsilon_c^5=0 \tag{86}$$

and it must satisfy the condition $\varepsilon_c\leqslant\varepsilon_{z0}\leqslant\varepsilon_M$, where ε_M is the maximum value of ε_{z0}. For $u=1$, we have $\varepsilon_{z0}=\varepsilon_c$. It

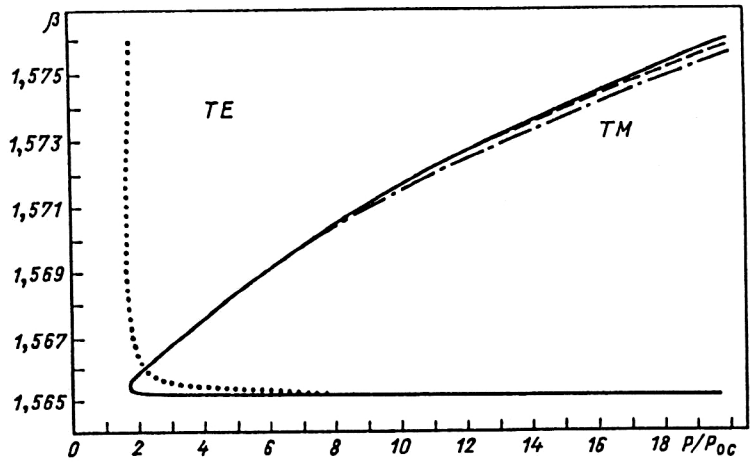

FIG. 22. Dependence of the effective refractive index β on the dimensionless energy flux P/P_{0c} for TE and TM waves. The parameters of the calculation are $n_c = 1.55$, $n_1 = 1.56$, $n_2 = 1.57$, and $d_1 = d_2 = \lambda$. The dotted curve is for the TE wave; the continuous curve corresponds to thermal nonlinearity; the broken curve corresponds to nonlinearity due to electronics; and the chain curve corresponds to nonlinearity due to molecular orientation.

can be shown that for $0 < u^2 \leqslant 1$ there exists a unique solution $\varepsilon_{z0} \geqslant \varepsilon_c$ [see Eq. (86)]. Moreover, for $u > 0$ we have

$$\operatorname{sign}\left(\frac{d\varepsilon_{zz}}{dz}\right) = 1.$$

For $u < 1$,

$$\operatorname{sign}\left(\frac{d\varepsilon_{zz}}{dz}\right) = \begin{cases} 1, & z < z_M, \\ -1, & z > z_M, \end{cases}$$

where z_M is the position of the maximum value of $\varepsilon_{zz}(z)$.

The upshot is

$$P_{NL} = \frac{\beta}{2\mu_0 c} \int_{\varepsilon_0}^{\varepsilon_{z0}} \varepsilon_{zz}^{-1} \left[\operatorname{sign}\left(\frac{d\varepsilon_{zz}}{dz}\right)\right] [F(\varepsilon_{zz})]^{-1/2} \frac{\mu_0}{\varepsilon_0} H_y^2 d\varepsilon_{zz}$$

$$= \frac{P_0}{2\beta^2(1-\gamma^2)} \left[\int_{\varepsilon_c}^{\varepsilon_{z0}} R(\varepsilon_{zz}) d\varepsilon_{zz} + (1 - \operatorname{sign} u) \int_{\varepsilon_{z0}}^{\varepsilon_M} R(\varepsilon_{zz}) d\varepsilon_{zz} \right], \tag{87}$$

where $P_0 = (2\alpha_c k_0)^{-1} (\varepsilon_0/\mu_0)^{1/2}$ and

$$R(\varepsilon_{zz}) = \frac{\varepsilon_{zz}}{\varepsilon_{xx}} \left[\frac{\varepsilon_{zz} - \gamma\varepsilon_{xx} - (1-\gamma)\varepsilon_s}{\varepsilon_{xx} - \gamma\varepsilon_{zz} - (1-\gamma)\varepsilon_s}\right]^{1/2} \left[2(\varepsilon_{zz} - \varepsilon_s) - 2\gamma(\varepsilon_{xx} - \varepsilon_s) + \varepsilon_{zz}\left(1 - \gamma\frac{d\varepsilon_{xx}}{d\varepsilon_{zz}}\right)\right]. \tag{88}$$

In the limit $\gamma \to 1$, i.e., when the nonlinearity is due to thermal effects or electrostriction effects, we obtain the results of Ref. 9 from the above expressions. Figure 22 shows the nonlinear dispersion curves for the TE and TM waves. Note that in the considered case there is no linear limit for either wave type, and their difference must be taken into

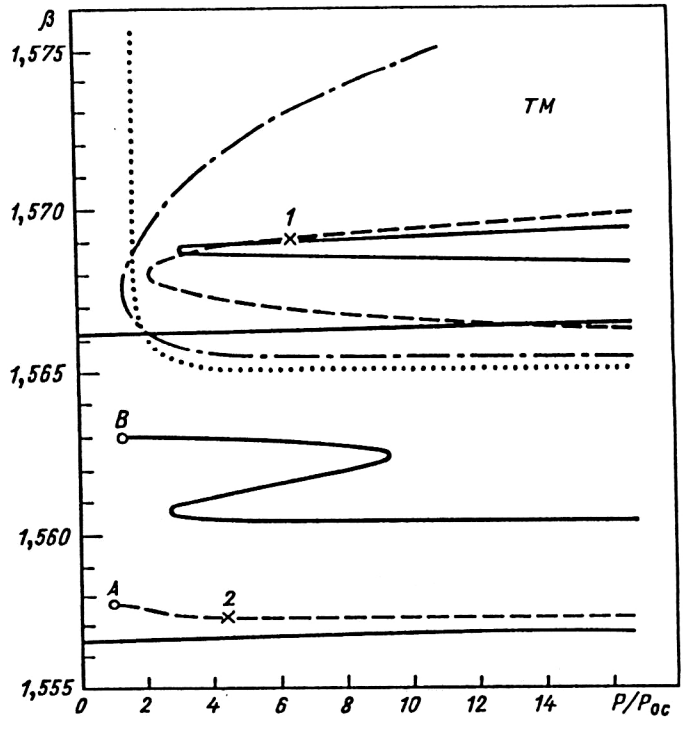

FIG. 23. Dependence of the effective refractive index β on the dimensionless energy flux P/P_0 in the case of thermal nonlinearity. The parameters of the calculation are $n_c = 1.55$, $n_1 = 1.57$, $n_2 = 1.56$, $d_1 = d_2 = \delta\lambda$. The dotted curve is for $\delta = 0.05$, the chain curve for $\delta = 1$, the broken curve for $\delta = 2$, and the continuous curves for $\delta = 3$.

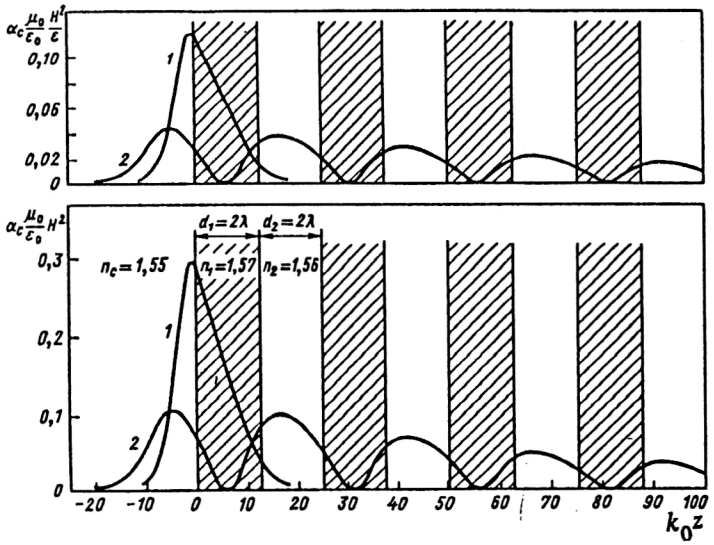

FIG. 24. Dependence of $\alpha(\mu_0/\varepsilon_0)(H^2/\varepsilon)$ and $\alpha(\mu_0/\varepsilon_0)H^2$ on the dimensionless quantity k_0z. The parameters of the calculation are $n_c = 1.55$, $n_1 = 1.57$, $n_2 = 1.56$, $d_1 = d_2 = 2\lambda$. Curve 1 is for $\beta = 1.569$, and curve 2 is for $\beta = 1.5572$.

account. In the case of *TM* waves, there is no particular difference between the results corresponding to the different nonlinearity mechanisms. The theoretical approach presented here makes it possible to obtain results similar to the numerical results of Ref. 11 in the description of the propagation of nonlinear surface waves between nonlinear and linear dielectrics. Figure 23 shows the nonlinear dispersion curves for *TM* waves in the case of nonlinearity due to thermal effects or electrostriction effects ($\gamma = 1$) when the thicknesses of the layers are chosen in accordance with $d_1 = d_2 = \delta\lambda$. For $\delta = 0.05$ and $\delta = 1.0$, we have propagation of *TM* waves when a certain threshold value of the energy flux is exceeded. For $\delta = 2$, there are two branches of the nonlinear dispersion curve, which do not have a linear limit and are separated by a region of forbidden values of β. The number of different branches of the nonlinear dispersion curves increases with increasing thickness d of the cell of the periodic structure. For example, for $\delta = 3$ there are four branches, two of which have a linear limit.

Figure 24 shows $\alpha_c = (\mu_0/\varepsilon_c)(H^2/\varepsilon)$ and $\alpha_c = (\mu_0/\varepsilon_c)H^2$ as functions of the dimensionless coordinate k_0z for two values of β. For a value of β corresponding to positive slope of the upper branch of the nonlinear dispersion curve (point 1 in Fig. 23), there exists only one maximum of the optical field, which is concentrated at the boundary surface between the self-focusing cladding and the linear superlattice. For $\beta = 1.5572$ (point 2 in Fig. 23), one maximum is in the nonlinear cladding, and the others are localized in each cell of the periodic layered structure. Figure 25 shows the nonlinear dispersion curves for *TM* waves for the same nonlinearity as in Fig. 23 but for other parameters of the structure. For $\delta = 0.2$, a linear limit of the nonlinear dispersion curve does not exist. For $\delta = 0.5$, 1, and 1.5, linear solutions exist at zero value of the energy flux. However, for $\delta = 1.5$ there exist three different values of the propagation constant β for given value of the energy flux. This property can be used in the design of integrated all-optical devices as switches.

Nonlinear guided waves in finite multilayer periodic struc tures contiguous with nonlinear self-focusing media

We consider a multilayer dielectric structure consisting of: a semi-infinite nonlinear self-focusing medium of Kerr type characterized by dielectric function $\varepsilon = \varepsilon_s + \alpha_s|\mathbf{E}|^2$ ($\alpha_s > 0$) in the region $z < 0$; a linear dielectric structure of step profile consisting of N cells, each made of materials 1 and 2 of thicknesses d_1 and d_2, respectively, and character-

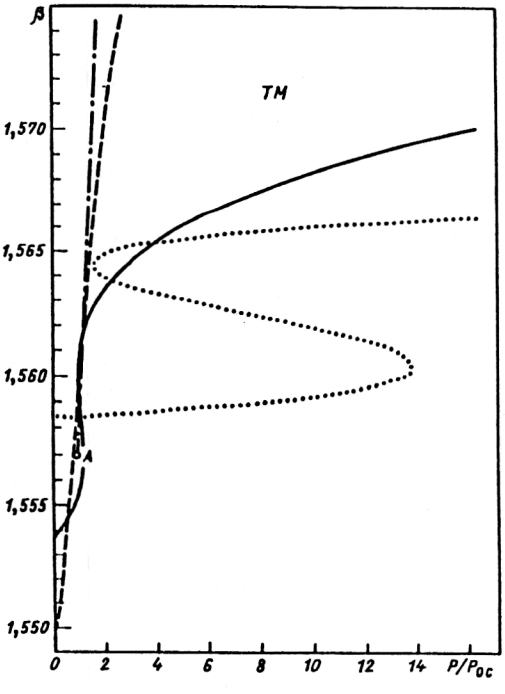

FIG. 25. The same as in Fig. 23. The chain curve is for $\delta = 0.2$, the broken curve for $\delta = 0.5$, the continuous curve for $\delta = 1$, and the dotted curve for $\delta = 1.5$.

ized by dielectric constants ε_1 and ε_1 in the region $0<z<N(d_1+d_2)$; and a semi-infinite nonlinear self-focusing cladding of Kerr type characterized by dielectric function $\varepsilon=\varepsilon_c+\alpha_c|\mathbf{E}|^2$ $(\alpha_c>0)$ in the region $z>N(d_1+d_2)$.

Maxwell's equations for TE polarized waves propagating along the x axis have the form

$$\frac{d^2E_y}{dz^2}-k_0^2q_s^2E_y+\alpha_sk_0^2E_y^3=0, \quad z<0; \tag{89}$$

$$\frac{d^2E_y}{dz^2}-k_0^2q_1^2E_y=0, \quad nd<z<nd+d_1; \tag{90}$$

$$\frac{d^2E_y}{dz^2}-k_0^2q_2^2E_y=0, \quad nd+d_1<z<(n+1)d; \tag{91}$$

$$\frac{d^2E_y}{dz^2}-k_0^2q_0^2E_y+\alpha_ck_0^2E_y^3=0, \quad z>Nd, \tag{92}$$

where $q_i^2=\beta^2-\varepsilon_i$, $i=s,1,2,c,d=d_1+d_2$, $n=0,1,2,...,N-1$. Integrating Eqs. (89) and (92) with allowance for the condition $E_y\to 0$ as $z\to\pm\infty$, we obtain the following solutions for the substrate and cladding:

$$E_y(z)=\left(\frac{2}{\alpha_s}\right)^{1/2}q_s\{\cosh[k_0q_s(z-z_s)]\}^{-1}, \quad z<0; \tag{93}$$

$$E_y(z)=\pm\left(\frac{2}{\alpha_s}\right)^{1/2}q_s\{\cosh[k_0q_c(z-z_s)]\}^{-1}, \quad z>Nd, \tag{94}$$

where z_s and z_c are integration parameters, and $q_{s,c}=(\beta^2-\varepsilon_{s,c})^{1/2}$. For convenience, the field in the substrate is taken to be positive, $E_0=E_y(0)>0$. The integration parameters z_s and z_c, and also the sign in the expression (94), are determined from the boundary conditions at $z=0$ and $z=Nd$. We introduce two dimensionless quantities u_1 and u_2, which are associated with the values of the field at the boundaries $z=0$ and $z=Nd$:

$$u_1=(k_0q_s)^{-1}\left[\frac{d}{dz}\ln E_y\right]_{z=0}=\tanh(k_0q_sz_s) \tag{95}$$

and

$$u_2=(k_0q_c)^{-1}\left[\frac{d}{dz}\ln E_y\right]_{z=Nd}=\tanh[(k_0q_c(Nd-z_c)]. \tag{96}$$

Using u_1 and u_2, we can express the value of the field at the boundary by means of them:

$$E_0=\left(\frac{2}{\alpha_s}\right)^{1/2}q_s(1-u_1^2)^{1/2}; \quad E_N=\pm\left(\frac{2}{\alpha_c}\right)^{1/2}q_c(1-u_2^2)^{1/2}, \tag{97}$$

where $0\leqslant u_1^2\leqslant 1$ and $0\leqslant u_2^2\leqslant 1$. Note that for $\alpha_s=0$ and/or $\alpha_c=0$ (the case of a linear dielectric substrate and/or linear dielectric cladding) we have $u_1=1$ and/or $u_2=1$, so that the limits of E_0 and E_N in the general case are finite and nonzero.

The general solution of Maxwell's equations for a linear multilayer medium satisfying boundary conditions at $z=nd$ is determined by the relations (45) and (46). The coefficients A_n^c and A_n^s are determined by means of the boundary conditions at the surfaces $z=0$, $z=nd+d_1$ and $z=Nd$ and satisfy the relation

$$\begin{pmatrix}A_{n+1}^c\\A_{n+1}^s\end{pmatrix}=T\begin{pmatrix}A_n^c\\A_n^s\end{pmatrix}, \quad n=0,1,2,...,N-1, \tag{98}$$

where $A_0^c=E_0$, $A_0^s=q_su_1E_0$, $A_N^c=E_N$, $A_N^s=-q_cu_2E_N$, and the matrix T is determined by (48). From the recursion relations (98), we find

$$\begin{pmatrix}A_n^c\\A_n^s\end{pmatrix}=E_0T^n\begin{pmatrix}1\\q_su_1\end{pmatrix}; \quad \begin{pmatrix}A_n^c\\A_n^s\end{pmatrix}=E_NT^{(n-N)}\begin{pmatrix}1\\-q_cu_2\end{pmatrix}. \tag{99}$$

The eigenvalues and eigenvectors of T are determined by means of the expressions (49)–(52). If $\Delta\neq 0$, then $a_+\neq a_-$ and the column vector in the expression (99) can be represented by means of the linearly independent vectors $V_\pm$ of the transfer matrix T. Finally, we find

$$\begin{pmatrix}A_n^c\\A_n^s\end{pmatrix}=E_0s^nD\begin{pmatrix}A^-\exp(-ntk_0d)-A^+\exp(ntk_0d)\\A^-\exp(-ntk_0d)a_--A^+\exp(ntk_0d)a_+\end{pmatrix}; \tag{100}$$

$$\begin{pmatrix}A_n^c\\A_n^s\end{pmatrix}=E_Ns^{(N-n)}D\begin{pmatrix}B^-\exp(-(n-N)tk_0d)-B^+\exp(ntk_0d)\\B^-\exp(-(n-N)tk_0d)a_--B^+\exp((n-N)tk_0d)a_+\end{pmatrix}; \tag{101}$$

where $A^{\pm}=a_{\mp}-q_s u_1$, $B^{\pm}=a_{\mp}+q_c u_2$, and $D=(a_+-a_-)^{-1}$. From Eqs. (100) and (101), we obtain the following relations for the dimensionless quantities u_1 and u_2:

$$\pm\left(\frac{2}{\alpha_c}\right)^{1/2} q_c(1-u_2^2)^{1/2} = s^N\left(\frac{2}{\alpha_s}\right)^{1/2} q_s(1-u_1^2)^{1/2} D[(a_+ - q_s u_1) \times \exp(-Ntk_0 d) - (a_- - q_s u_1)\exp(Ntk_0 d)]; \tag{102}$$

$$\pm\left(\frac{2}{\alpha_c}\right)^{1/2} q_c(1-u_2^2)^{1/2} u_2 = -s^N\left(\frac{2}{\alpha_s}\right)^{1/2} q_s(1-u_1^2)^{1/2} D[(a_+ - q_s u_1)a_- \times \exp(-Ntk_0 d) - (a_- - q_s u_1)a_+ \exp(Ntk_0 d)]. \tag{103}$$

As a result, we have

$$(\pm)=s^N \operatorname{sign}[D(q_s u_1 a_1 - a_2)]; \tag{104}$$

$$u_2 = -\frac{a_+ a_- a_1 - q_s u_1 a_3}{q_c(a_2 - q_s u_1 a_1)}, \tag{105}$$

where u_1 is determined from the solution of the equation

$$a_1^4 a_+ q_s^6 u_1^6 - 4a_1^3 a_2 a_4 q_s^5 u_1^5 + a_1^2(6a_2^2 - q_s^2 a_1^2)a_4 q_s^4 u_1^4 + 4a_1 a_2(a_1^2 q_s^2 - a_2^2)a_4 q_s^3 u_1^3 + [(a_2^2 - 6a_1^2 q_s^2)a_2^2 a_4 + q_c^2 a_1^2 - a_3^2]q_s^2 u_1^2 + 2a_1(2a_2^3 a_4 q_s^2 + a_3 a_+ a_- - a_2 q_c^2) q_s u_1 - a_2 a_4 q_s^2 + a_2^2 q_2^c - a_+^2 a_-^2 a_1^2 = 0. \tag{106}$$

Here

$$a_1 = \exp(Ntk_0 d) - \exp(-Ntk_0 d);$$

$$a_{2,3} = a_{\mp}\exp(Ntk_0 d) - a_{\pm}(-Ntk_0 d) \text{ and}$$

$$a_4 = \alpha_c D^2/\alpha_2.$$

Solving the sixth-order equation (106) for the unknown u_1, and then substituting the solution in Eq. (105), we determine u_2. We must expect several solutions for u_1 and u_2 in the region of physical values $-1 \leqslant u_1(u_2) \leqslant 1$ for fixed value of the effective refractive index β. As in the case of a linear dielectric film surrounded on two sides with a nonlinear medium when both the linear and the nonlinear symmetry is broken ($n_s \neq n_c$ or $\alpha_c \neq \alpha_s$), several values can exist for the propagation constants (Refs. 1, 3, 4, 72, and 73).

The flux of energy transported by the electromagnetic wave is determined by means of the Poynting vector as follows:

$$P=\frac{\beta}{2\mu_0 c}\int_{-\infty}^{\infty} E_y^2(z)dz = P_s + P_{MLS} + P_c, \tag{107}$$

where P_s, P_{MLS}, and P_c are the parts of the energy flux in the nonlinear substrate, in the infinite linear multilayer structure, and in the nonlinear cladding, respectively:

$$P_s = 2P_{0s}(1-u_1)q_s; \tag{108}$$

$$P_c = 2P_{0c}(1-u_2)q_c; \tag{109}$$

$$P_{MLS}=P_{0s}\beta q_s^2(1-u_1^2)D^2\left[\frac{1-\exp(-2Ntk_0 d)}{1-\exp(-2tk_0 d)}(a_+ - q_s u_1)^2 F_1^- + \frac{\exp(2Ntk_0 d)-1}{\exp(2tk_0 d)-1}(a_- - q_s u_1)^2 F_1^+ - 2N(a_+ - q_s u_1)(a_- - q_s u_1)F_1\right] + P_{0c}\beta q_c^2(1-u_2^2)D^2\left[\frac{1-\exp(-2Ntk_0 d)}{1-\exp(-2tk_0 d)}(a_- + q_c u_2)^2 F_2^+ + \frac{\exp(2Ntk_0 d)-1}{\exp(2tk_0 d)-1}(a_+ + q_c u_2)^2 F_2^- - 2N(a_- + q_c u_2)(a_+ + q_c u_2)F_2\right]. \tag{110}$$

Here

$$P_{0s,c}=(2a_{s,c}k_0)^{-1}(\varepsilon_0/\mu_0)^{1/2}$$

and

$$F_i = \frac{\cosh\gamma_i \sinh\gamma_i + \gamma_i}{q_i} + (-1)^{i+1}(a_+ + a_-)\times\left(\frac{\sinh\gamma_i}{q_i}\right)^2 + a_+ a_- \frac{\cosh\gamma_i \sinh\gamma_i - \gamma_i}{q_i^3} \quad (i=1,2); \tag{111}$$

$$F_i^{\pm} = \frac{\cosh\gamma_i \sinh\gamma_i + \gamma_i}{q_i} + (-1)^{i+1}2a_{\pm}\left(\frac{\sinh\gamma_i}{q_i}\right)^2 + a_{\pm}^2 \frac{\cosh\gamma_i \sinh\gamma_i - \gamma_i}{q_i^3} \quad (i=1,2). \tag{112}$$

Figure 26 shows the nonlinear dispersion curves for the case $n_s = n_c$ and $\alpha_s = 2\alpha_c$. For TE_0 nonlinear guided waves

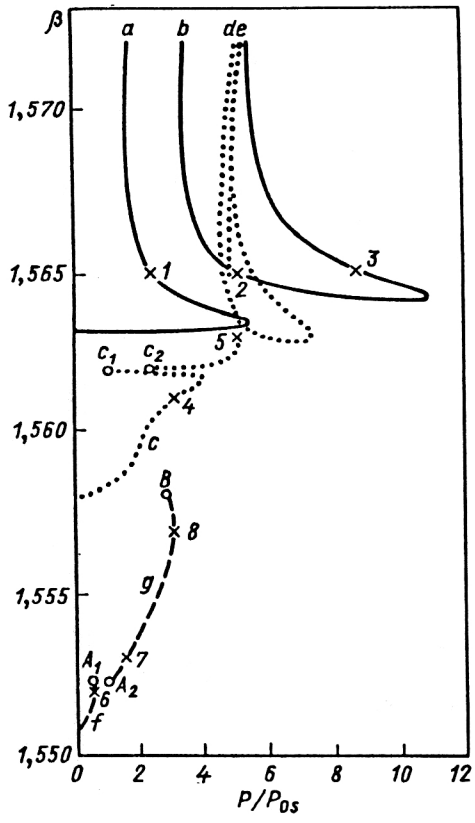

FIG. 26. Dependence of the effective refractive index β on the dimensionless energy flux P/P_{0s}. The parameters of the calculation are $n_s = 1.55$, $n_1 = 1.57$, $n_2 = 1.56$, $n_c = 1.55$, $\alpha_c/\alpha_s = 0.5$, $d_1 = d_2 = 0.5\lambda$, and $N = 5$. The continuous curves are for the TE_0 branches, the dotted curves for the TE_1 branches, and the broken curves for the TE_2 branches.

there exist two disconnected branches (a and b in Fig. 26), one of which (b) exists only above a certain threshold value of the energy flux. In the case $\alpha_c \neq \alpha_s$, there exist three independent branches c, d, and e for TE_1 waves, of which branches d and e have threshold behavior; there are two branches f and g for TE_2 waves, one of which (branch g) also has threshold behavior.

Figure 27 shows the square of the dimensionless amplitude $|A|^2 = \alpha_s |E_y(z)|^2$ as a function of the dimensionless coordinate $k_0 z$ for three values of the energy flux corresponding to the same effective refractive index $\beta = 1.565$ (points 1–3 on the nonlinear dispersion curve). Branch a develops from the linear limit (see Fig. 26), and the corresponding optical field is localized in the more nonlinear medium, namely, in the substrate (curve 1 in Fig. 27). The field maximum corresponding to the second branch (branch b in Fig. 26) starts from the medium with lesser nonlinearity, from the cladding (the corresponding profile of the optical field is shown by curve 2 in Fig. 27). The profile of the optical field in the linear multilayer structure has an oscillatory nature (curve 3 in Fig. 27) when the corresponding maxima are localized in each unit cell of the periodic dielectric structure. Figure 28 shows the behavior of $|A|^2$ for points 4 and 5 of the branches of the nonlinear dispersion curve (see Fig. 26). Note that there are local field maxima in the multilayer structure. At the same time, the maximum of the first branch of the TE_1 wave (branch c in Fig. 26), situated near the contiguous substrate, moves with increasing $k_0 z$ into the contiguous medium (curve 4 in Fig. 28). The maxima of the second branch of the TE_1 wave (branch d in Fig. 26) are situated asymmetrically in the two nonlinear media (curve 5 in Fig. 28) with stronger localization in the medium with lesser nonlinearity (the cladding). Figure 29 shows the square of the field amplitude $|A|^2$ as a function of the dimensionless coordinate $k_0 z$ for three different values of the effective refractive index β (points 6–8 of the nonlinear dispersion curve in Fig. 26). Branch f, which starts from the linear limit, terminates at the point A_1. Accordingly, for this branch there are two local maxima in the multilayer structure and one field extremum in the self-focusing substrate (curve 6 in Fig. 29). The second branch of the TE_2 wave (branch g in Fig. 26) begins at the point A_2 and terminates at the point B. One of the three maxima of the field profile corresponding to the behavior of branch g near the termination point A_2 is in the medium with smallest nonlinearity (the cladding) (curve 7 in Fig. 29). Two of the three maxima of the field profile corresponding to the behavior of branch g near the termination point B are localized in the two nonlinear boundary media (curve 8 in Fig. 29).

For $n_s = n_s$ and $\alpha_c = \alpha_s$ we observe (Fig. 30) two branches a and b of the TE_0 wave, one of which (b) has threshold behavior; there are two branches c and d of the TE_1 wave, the latter (d) having a threshold of the energy flux; finally, there is one TE_2 wave (branch e), which develops from the linear limit. In this case, since the two contiguous media possess the same self-focusing nonlinearities, the branches a and b are coupled.

We consider the propagation of TM polarized nonlinear guided waves in a finite periodic medium with step profile contiguous with an isotropic nonlinear cladding of Kerr type and a linear dielectric substrate. Suppose we have a multilayer structure of the following type: semi-infinite optically isotropic cladding of Kerr type characterized by dielectric function $\varepsilon = \varepsilon_c + \alpha_c |\mathbf{E}|^2$ ($\alpha_c > 0$) in the region $z > 0$; a linear periodic structure consisting of N cells that each contains layers of materials 1 and 2 of thickness d_1 and d_2, respectively, and characterized by dielectric constants ε_1 and ε_2 in the region $0 < z < N(d_q + d_2)$; and a semi-infinite linear substrate characterized by dielectric constant ε_s in the region $z > N(d_1 + d_2)$. The general solution of Maxwell's equations in the linear periodic structure is determined by the relations (63) and (64). In the linear substrate, we have the exponential solution

$$H_y(z) = H_N \exp[-k_0 q_s (z - Nd)], \tag{113}$$

where $q_s = (\beta^2 - n_s^2)^{1/2}$, and H_N will be determined by means of the boundary conditions at the surface $z = Nd$. Introducing the dimensionless parameter u,

$$u=\frac{\varepsilon_c}{k_0 q_c H_0}\left[\frac{1}{\varepsilon}\frac{dH_y}{dz}\right]_{z=0}, \tag{114}$$

where $H_0=H_y(0)$ and $q_c=(\beta^2-n_c^2)^{1/2}$, we obtain by means of the boundary conditions on the surfaces $z=0$ and $z=Nd$ the following relations for the amplitudes A_n^c and A_n^s:

$$\begin{pmatrix}A_0^c\\A_0^s\end{pmatrix}=H_0\begin{pmatrix}1\\u\dfrac{q_c}{\varepsilon_c}\end{pmatrix};\quad \begin{pmatrix}A_N^c\\A_N^s\end{pmatrix}=H_N\begin{pmatrix}1\\-\dfrac{q_s}{\varepsilon_s}\end{pmatrix}. \tag{115}$$

Using the transfer-matrix method, we obtain the necessary expressions for the parameter u and the field amplitude at the boundary $z=Nd$; in final form, they are

$$u=\frac{\varepsilon_c}{q_c}\frac{\left(\frac{q_s}{\varepsilon_s}+b_+\right)b_-\exp(Ntk_0d)-\left(\frac{q_s}{\varepsilon_s}+b_-\right)b_+\exp(-Ntk_0d)}{\left(\frac{q_s}{\varepsilon_s}+b_+\right)\exp(Ntk_0d)-\left(\frac{q_s}{\varepsilon_s}+b_-\right)\exp(-tk_0d)}; \tag{116}$$

$$H_N=\frac{s^N(b_+-b_-)H_0}{\left(\frac{q_s}{\varepsilon_s}+b_+\right)\exp(Ntk_0d)-\left(\frac{q_s}{\varepsilon_s}+b_-\right)\exp(-Ntk_0d)}. \tag{117}$$

Here, $b_\pm$ are determined by the relations (70). The total energy flux is $P=P_s+P_f+P_c$, where P_s, P_f, and P_c are the corresponding energy fluxes in the linear substrate, in the finite periodic structure, and in the nonlinear cladding. The energy fluxes in the periodic structure and in the linear substrate are determined by expressions of the form

$$\begin{aligned}P_f=P_0\beta g&\left[\left(\frac{q_s}{\varepsilon_s}+b_+\right)\exp(Ntk_0d)-\left(\frac{q_s}{\varepsilon_s}+b_-\right)\exp(-Ntk_0d)\right]^{-2}\left[\left(\frac{q_s}{\varepsilon_s}+b_+\right)^2\right.\\&\times[G_1^-+\exp(-2tk_0d)G_2^-]\frac{\exp(2Ntk_0d)-1}{1-\exp(-2tk_0d)}+\left(\frac{q_s}{\varepsilon_s}+b_-\right)^2[G_1^++\exp(2tk_0d)G_2^+]\\&\left.\times\frac{1-\exp(-2Ntk_0d)}{\exp(2tk_0d)-1}-2N(G_1+G_2)\left(\frac{q_s}{\varepsilon_s}+b_-\right)\left(\frac{q_s}{\varepsilon_s}+b_+\right)\right];\end{aligned} \tag{118}$$

$$P_s=\frac{P_0\beta g}{\varepsilon_s q_s}(b_+-b_-)^2\left[\left(\frac{q_s}{\varepsilon_s}+b_+\right)\exp(Ntk_0d)-\left(\frac{q_s}{\varepsilon_s}+b_-\right)\exp(-Ntk_0d)\right]^{-2}. \tag{119}$$

Here

$$P_0=(2\alpha_c k_0)^{-1}(\varepsilon_0/\mu_0)^{1/2};$$

$$G_i^\pm=\frac{\cosh\gamma_i\sinh\gamma_i+\gamma_i}{\varepsilon_i q_i}+(-1)^{i+1}2b_\pm\left(\frac{\sinh\gamma_i}{q_i}\right)^2+\varepsilon_i b_\pm^2\frac{\cosh\gamma_i\sinh\gamma_i-\gamma_i}{q_i^3}\quad(i=1,2,); \tag{120}$$

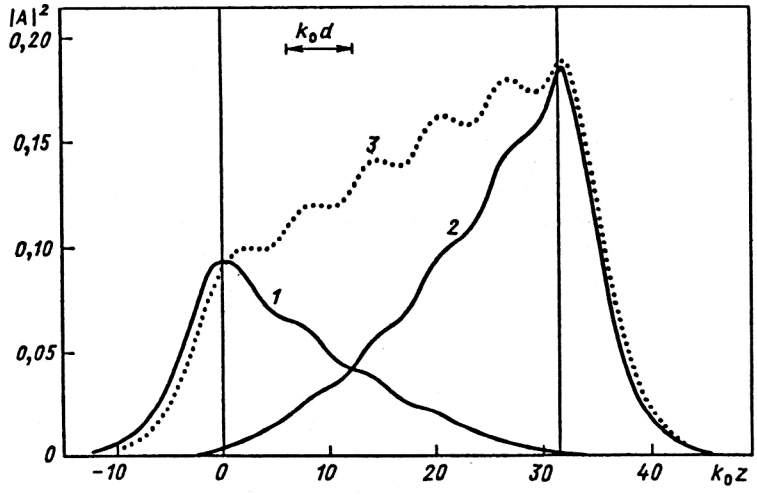

FIG. 27. Dependence of the square $|A|^2$ of the field amplitude on the dimensionless quantity k_0z for the three points 1, 2, and 3 of the branches of the TE_0 wave in Fig. 26 for $\beta=1.565$.

$$G_i=\frac{\cosh\gamma_i\sinh\gamma_i+\gamma_i}{\varepsilon_i q_i}+(-1)^{i+1}(b_++b_-)\left(\frac{\sinh\gamma_i}{q_i}\right)^2+\varepsilon_i b_+b_-\frac{\cosh\gamma_i\sinh\gamma_i-\gamma_i}{q_i^3}\quad(i=1,2);\tag{121}$$

$$g=\frac{\varepsilon(0)[\varepsilon^2(0)-\varepsilon_c^2]}{4[2\beta^2-\varepsilon(0)]},\tag{122}$$

where $\varepsilon(0)$ is the value of the dielectric function $\varepsilon(z)=\varepsilon_c+\alpha_c|\mathbf{E}|^2$ of the nonlinear cladding at the boundary $z=0$.[51]

The energy flux in the nonlinear cladding can be calculated exactly:[9,50]

$$P_c=\frac{P_0\beta}{2}\left[\int_{\varepsilon_c}^{\varepsilon(0)}I(\varepsilon)d\varepsilon+(1-\operatorname{sign}u)\int_{\varepsilon(0)}^{\varepsilon_M}I(\varepsilon)d\varepsilon\right],\tag{123}$$

where

$$I(\varepsilon)=\frac{(\varepsilon+\varepsilon_c)^{1/2}(3\beta^2\varepsilon^2-\varepsilon^3-\beta^2\varepsilon_c^2)}{\varepsilon(2\beta^2-\varepsilon)^2(3\beta^2\varepsilon-2\varepsilon^2-\beta^2\varepsilon_c)^{1/2}}.\tag{124}$$

The quantity $\varepsilon(0)$ is determined from the equation

$$;9q\varepsilon^3(0)(\beta^2-\varepsilon_c)u^2+\varepsilon^2(0)[(\beta^2-\varepsilon_c)\varepsilon_c u^2+2\varepsilon_c^2]$$

$$-3e(0)\beta^2\varepsilon_c^2+\beta^2\varepsilon_c^3=0.\tag{125}$$

The physical solutions for $\varepsilon(0)$ must satisfy the condition $\varepsilon_c\leqslant\varepsilon(0)\leqslant\varepsilon_M$, where ε_M is the possible maximal value of the dielectric function $\varepsilon(z)$ for the nonlinear cladding; it is determined from the condition $d\varepsilon/dz=0$, i.e.,

$$\varepsilon_M=\tfrac{3}{4}[\beta^2+\beta(\beta^2-\tfrac{8}{9}\varepsilon_c)^{1/2}].$$

For TE polarized nonlinear guided waves propagating in an analogous multilayer dielectric structure, we obtain by means of the transfer-matrix method the following expressions for the dimensionless parameter u and for the field at the boundary $z=Nd$:[52]

$$u=\frac{(q_s+a_+)a_-\exp(Ntk_0d)-(q_s+a_-)a_+\exp(-Ntk_0d)}{q_c[(q_s+a_+)\exp(Ntk_0)-(q_s+a_-)\exp(-Ntk_0d)]};\tag{126}$$

$$E_N=\frac{s^N(a_+-a_-)E_0}{(q_s+a_+)\exp(Ntk_0d)-(q_s+a_-)\exp(-Ntk_0d)}.\tag{127}$$

The total energy flux $P=P_s+P_f+P_c$ is determined by means of the expressions[52]

$$P_c=2P_0\beta q_c(1-u);\tag{128}$$

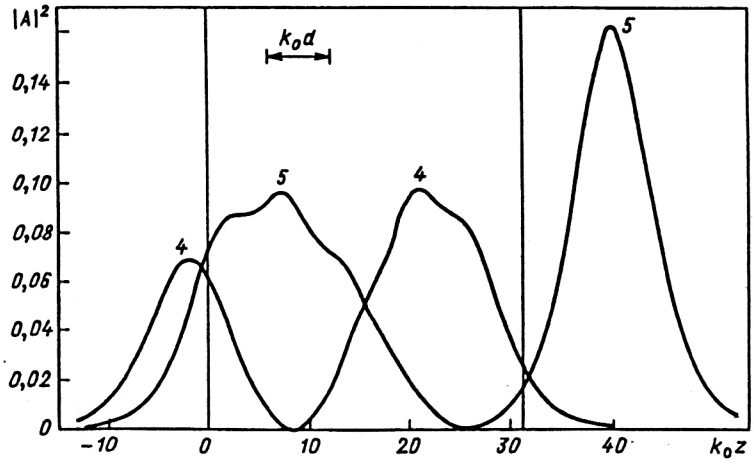

FIG. 28. The same as in Fig. 27 for the points 4 and 5 of the branches of the TE_1 wave in Fig. 26: $\beta=1.561$ (point 4 of the nonlinear dispersion curve) and $\beta=1.563$ (point 5 of the curve).

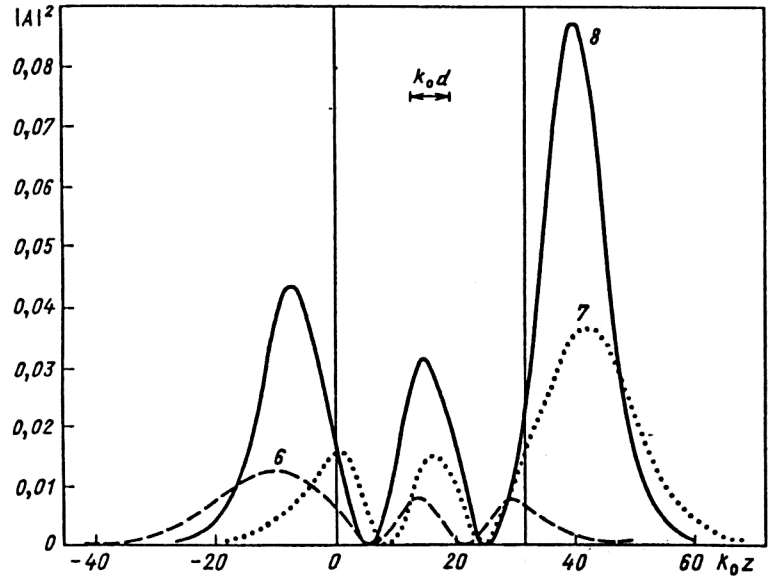

FIG. 29. The same as in Fig. 27 for the points 6, 7, and 8 of the branches of the TE_2 wave in Fig. 26. The broken curve is for $\beta = 1.522$ (point 6 of the nonlinear dispersion curve), the dotted curve is for $\beta = 1.563$ (point 7 of the curve), and the continuous curve is for $\beta = 1.567$ (point 8 of the curve).

$$P_f = P_0\beta q_c^2(1-u^2)[(q_s+a_+)\exp(Ntk_0d) - (q_s+a_-)\exp(-Ntk_0d)]^{-2}[(q_s+a_+)^2(F_1^- + \exp(-2tk_0d)F_2^-)$$
$$\times\frac{\exp(2Ntk_0d)-1}{1-\exp(-2tk_0d)} + (q_s+a_-)^2(F_1^+ + \exp(2tk_0d)F_2^+)\frac{1-\exp(-2Ntk_0d)}{\exp(2tk_0d)-1}$$
$$-2N(F_1+F_2)(q_s+a_-)(q_s+a_+)]; \tag{129}$$

$$P_s = P_0\beta(1-u^2)\frac{q_c^2}{q}(a_+ - a_-)^2[(q_s+a_+)\exp(Ntk_0d) - (q_s+a_-)\exp(-Ntk_0d)]^{-2}, \tag{130}$$

where F_i and $F_i^{\pm}$ are determined by the expressions (111) and (112). Figure 31 shows the results of calculation of the nonlinear dispersion curves for TM waves when the nonlinearity is due to thermal effects or electrostriction effects ($\gamma = 1$). A characteristic feature of the solution for TM_0 nonlinear guided waves is the presence of propagation of the optical field for $\beta > \max(n_1, n_2)$ and the existence of a local maximum in the energy flux of the directed wave (branch $\underline{a}$ in Fig. 31). The self-focusing effect of the nonlinear substrate leads to a maximum of the field in this medium, and the branches ($\underline{a}$) of the nonlinear guided waves degenerate at large values of the flux into a solitary surface wave. Self-focusing in the nonlinear substrate also occurs for the higher orders of the solution for nonlinear guided waves (branch b in Fig. 31). We note that the values of the local maxima are clearly separated both for branches (a) and branches (b) for two different values of the refractive indices of the material. Figure 32 shows the nonlinear dispersion curves for the TE waves for different numbers N of cells. For $N=10$ and $N=20$, we have, respectively, two and four branches of nonlinear guided waves. It is worth mentioning that the branches of higher order terminate at a finite value of the energy flux when $\beta < \max(n_1, n_2)$ (the termination points A, B, C, and D in

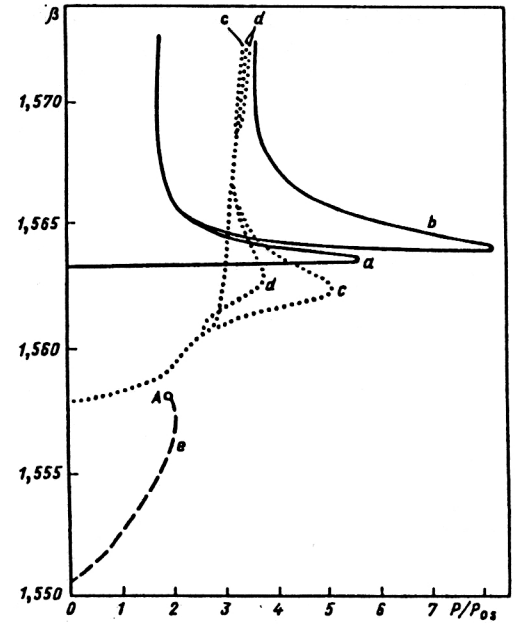

FIG. 30. The same as in Fig. 26 for $\alpha_c = \alpha_s$. The broken curves are for the TE_0 branch, the dotted curves are for the TE_1 branch, and the broken curve is for the TE_2 branch.

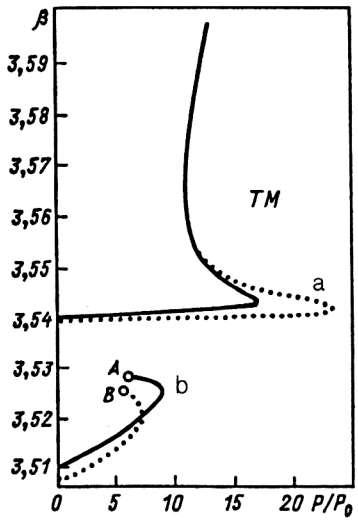

FIG. 31. Dependence of the effective refractive index β on the dimensionless energy flux P/P_0. The parameters of the calculation are $n_c = 3.502$, $n_s = 1$, $d_1 = d_2 = 0.075\lambda$, and $N = 10$; a) the continuous curve is for $n_1 = 3.59$, $n_2 = 3.513$; b) the dotted curve is for $n_1 = 3.513$, $n_2 = 3.59$.

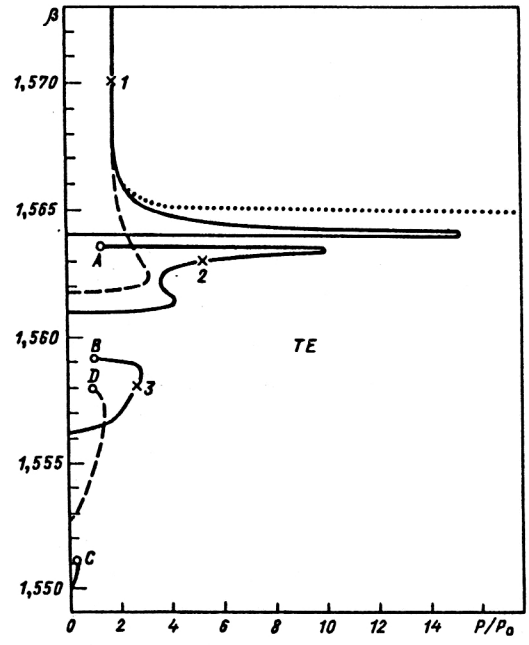

FIG. 32. The same as in Fig. 31. The parameters of the calculation are $n_c = 1.55$, $n_1 = 1.57$, $n_2 = 1.56$, $n_s = 1$, $d_1 = d_2 = 0.2\lambda$, $N = 10$ (broken curve), $N = 20$ (continuous curve), and $N = \infty$ (dotted curve).

Fig. 32). In the limit $N \to \infty$, we have only one branch (the dotted curve in Fig. 32), which corresponds to propagation of nonlinear surface waves at the interface between the nonlinear cladding and the semi-infinite periodic dielectric structure.

Figure 33 shows the field profile (the value of $|A|^2$) as a function of $k_0 z$ for $N = 20$ and three values of the propagation constant β. For point 1 on the nonlinear dispersion curve (Fig. 32) the field maximum is localized in the nonlinear self-focusing cladding. For point 2 on the nonlinear dispersion curve, we have two maxima of the nonlinear guided waves of first order, one of which is displaced to the region of the self-focusing cladding. For point 3 of the nonlinear dispersion curve for the branch of second order we have three field maxima, one of which is localized in the nonlinear cladding.

CONCLUSIONS

Investigations into the propagation of nonlinear guided waves represent one of the most strongly developing directions of integrated optics. This direction has great potential applications, both in the field of surface spectroscopy and in the development of optical information systems. As a rule, integrated all-optical systems combine a semiconductor laser as source operated in the milliwatt range, low-loss fiber coupling elements, and optical elements that can modulate, amplify, switch, limit, and operate in that power range in a picosecond time interval. The optical processor systems have the following advantages: (a) optical signals can remain optical; (b) wide bands, which permit transmission of short picosecond pulses; (c) a high transmission

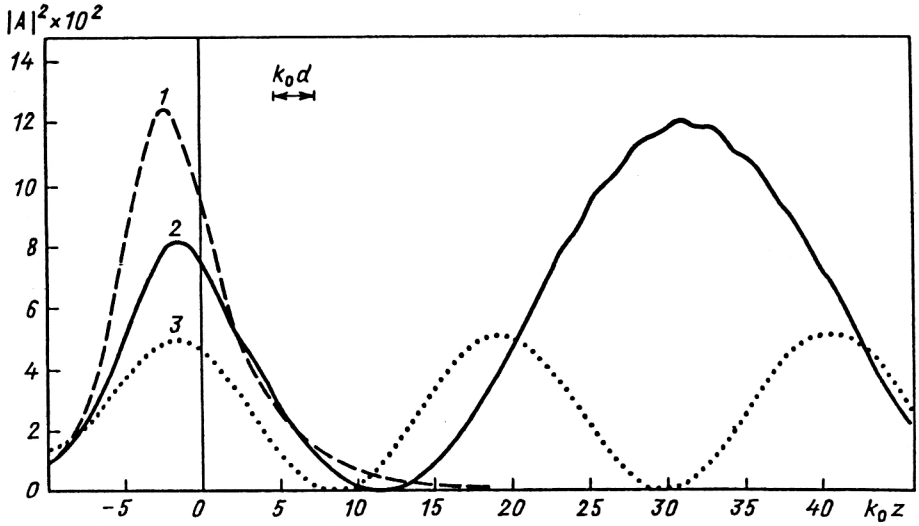

FIG. 33. Dependence of the square $|A|^2$ of the field amplitude on the dimensionless quantity $k_0 z$ for $N = 20$. The broken curve is for $\beta = 1.57$ (point 1 on the nonlinear dispersion curve in Fig. 32), the continuous curve is for $\beta = 1.563$ (point 2 on the curve), and the dotted curve is for $\beta = 1.558$ (point 3 on the curve).

rate of order 10^{-12}–10^{-14} sec. However, the currently existing materials restrict the experimental realization of the phenomenon of propagation of nonlinear guided waves. The optical nonlinearity of the material must be sufficient for the use of optical devices at milliwatt powers. In addition, in the case of switching the relaxation time of the induced nonlinear polarization must be measured in picoseconds. From this point of view, the most promising materials at the present time are the semiconductors GaAlAs and CdS_xSE_{1-x}, (SiO_2) glasses, and some other materials. We mention that the present status of the main problems and achievements in the development of the hardware of integrated optics for information transmission and analysis systems is described in the book of Ref. 74. The construction and use of integrated all-optical devices based on the propagation of nonlinear optical waves in layered structures should certainly lead to significant progress in the development of fiber-optic devices and integrated all-optical circuits, although there will be many serious engineering problems to solve.

[1] A. D. Boardman and P. Egan, in *Surface Waves in Plasmas and Solids*, edited by S. Vukovic (World Scientific, Singapore, 1986), p. 3.
[2] F. Lederer, U. Langbein, and H. E. Ponath, in *Lasers and their Applications*, edited by A. Y. Spassov (World Scientific, Singapore, 1987), p. 166.
[3] G. I. Stegeman *et al.*, J. Lightwave Techn. **6**, 953 (1988).
[4] D. Mihalache, R. G. Nazmitdinov, and V. K. Fedyanin, Fiz. Elem. Chastits At. Yadra **20**, 198 (1989) [Sov. J. Part. Nucl. **20**, 86 (1989)].
[5] A. G. Litvak and V. A. Mironov, Izv. Vyssh. Uchebn, Zaved, Radiofiz. **11**, 1911 (1986).
[6] V. M. Agranovich, V. S. Babichenko, and V. Ya. Chernyak, Pis'ma Zh. Eksp. Teor. Fiz. **32**, 532 (1980) [JETP Lett. **32**, 512 (1980)].
[7] A. A. Maradudin, Z. Phys. B **41**, 341 (1981).
[8] A. I. Lomtev, Pis'ma Zh. Eksp. Teor. Fiz. **34**, 64 (1981) [JETP Lett. **34**, 60 (1981)].
[9] K. M. Leung, Phys. Rev. B **32**, 5093 (1985).
[10] D. Mihalache *et al.*, Opt. Lett. **12**, 187 (1987).
[11] A. D. Boardman *et al.*, Phys. Rev. A **35**, 1159 (1987).
[12] N. N. Akhmediev, V. I. Korneev, and Yu. V. Kuz'menko, Zh. Eksp. Teor. Fiz. **88**, 107 (1985) [Sov. Phys. JETP **61**, 62 (1985)].
[13] A. V. Aceves, J. V. Moloney, and A. C. Newell, Phys. Rev. A **39**, 1809 (1989).
[14] Yu. S. Kivshar, A. M. Kosevich, and O. A. Chybykalo, Phys. Rev. A **41**, 1677 (1990).
[15] D. R. Heatley, E. M. Wright, and G. I. Stegeman, Appl. Phys. Lett. **53**, 172 (1988).
[16] G. Assanto, G. I. Stegeman, and G. Vitrant, Appl. Phys. Lett. **54**, 1854 (1989).
[17] G. Vitrant *et al.*, Opt. Lett. **14**, 898 (1989).
[18] N. N. Akhmediev, Zh. Eksp. Teor. Fiz. **83**, 545 (1982) [Sov. Phys. JETP **56**, 299 (1982)].
[19] V. K. Fedyanin and D. Mihalache, Z. Phys. B **47**, 167 (1982).
[20] D. Mihalache and V. K. Fedyanin, Teor. Mat. Fiz. **54**, 443 (1983).
[21] D. Mihalache, D. Mazilu, and H. Totia, Phys. Scr. **30**, 335 (1984).
[22] D. Mihalache, R. C. Nazmitdinov, and V. K. Fedyanin, Phys. Scr. **29**, 269 (1984).
[23] U. Langbein, F. Lederer, T. Peschel, and H. E. Ponath, Opt. Lett. **10**, 571 (1985).
[24] K. Hayata, O. Nagai, and M. Koshiba, IEEE Trans. Microwave Theory Tech. **36**, 1207 (1988).
[25] A. D. Boardman and T. Twardowski, Phys. Rev. A **39**, 2481 (1989).
[26] S. Vukovic and R. Dragila, Opt. Lett. **14**, 529 (1989).
[27] A. D. Boardman and P. Egan, IEEE J. Quantum Electron. **22**, 319 (1986).
[28] S. J. Al-Bader and H. A. Jamid, IEEE J. Quantum Electron. **23**, 1947 (1987).
[29] P. M. Lambkin and K. Allan Shore, IEEE J. Quantum Electron. **24**, 2046 (1988).
[30] N. N. Akhmediev, R. F. Nabiev, and Yu. M. Popov, Opt. Commun. **72**, 190 (1989).
[31] J. V. Moloney, J. Ariyasu, C. T. Seaton, and G. I. Stegeman, Appl. Phys. Lett. **L8**, 826 (1986).
[32] L. Leine, C. Wachter, U. Langbein, and F. Lederer, Opt. Lett. **12**, 747 (1987).
[33] D. Mihalache *et al.*, Phys. Lett. **129A**, 473 (1988).
[34] E. M. Wright, G. I. Stegeman, C. T. Seaton, and J. V. Moloney, Appl. Phys. Lett. **49**, 435 (1986).
[35] E. M. Wright *et al.*, Phys. Rev. A **34**, 4442 (1986).
[36] M. A. Gubbels *et al.*, J. Opt. Soc. Am. **B4**, 1837 (1987).
[37] D. R. Heatley, E. M. Wright, and G. I. Stegeman, Appl. Phys. Lett. **56**, 215 (1990).
[38] P. Yen, A. Yariv, and C. S. Hong, J. Opt. Soc. Am. **67**, 423 (1977).
[39] V. M. Agramovich and V. E. Kravtsov, Solid State Commun. **55**, 85 (1985).
[40] R. E. Wallis and J. J. Quinn, Phys. Rev. B **38**, 4205 (1988).
[41] P. Yen, in *Optical Waves in Layered Media* (Wiley, Chichester, 1988).
[42] S. D. Gupta, J. Opt. Soc. Am. **B6**, 1927 (1989).
[43] C. Martijn de Sterke and J. E. Sipe, Phys. Rev. A **38**, 5149 (1988).
[44] L. Kahn, N. S. Almedia, and D. L. Mills, Phys. Rev. B **37**, 8072 (1988).
[45] U. Trutschel and F. Lederer, J. Opt. Soc. Am. **B5**, 2530 (1988).
[46] A. I. Lomtev and L. G. Bol'shinskiĭ, Ukr. Fiz. Zh. **31**, 34 (1986).
[47] W. Chen and D. L. Mills, Phys. Rev. B **36**, 6268 (1987).
[48] M. Cadan, R. C. Gauthier, B. E. Paton, and J. Chrostowski, Appl. Phys. Lett. **49**, 755 (1986).
[49] U. Trutschel, F. Lederer, and M. Gotz, IEEE J. Quantum Electron. **25**, 194 (1989).
[50] D. Mihalache, D. Mazilu, and R. P. Wang, Solid State Commun. **69**, 685 (1989).
[51] D. Mihalache, R. P. Wang, and A. D. Boardman, Solid State Commun. **71**, 613 (1989).
[52] D. Mihalache, R. P. Wang, and A. D. Boardman, Phys. Lett. **138A**, 417 (1989).
[53] R. K. Varshney, M. A. Nehme, R. Srivastava, and R. V. Ramaswamy, Appl. Opt. **25**, 3899 (1986).
[54] K. Ogusu, Opt. Commun. **63**, 380 (1987).
[55] C. Wachter, U. Langbein, and F. Lederer, Appl. Phys. **B42**, 161 (1987).
[56] S. J. Al-Bader and H. A. Jamid, J. Opt. Soc. Am. **A5**, 374 (1988).
[57] L. Torner, F. Canal, and J. Hernandez-Marco, Opt. Quantum Electron. **21**, 451 (1989).
[58] R. K. Jain and R. C. Lind, J. Opt. Soc. Am. **73**, 647 (1983).
[59] S. D. Chemla, D. A. B. Miller, and P. W. Smith, Opt. Eng. **24**, 556 (1985).
[60] W. R. Holland, J. Opt. Soc. Am. **B3**, 1529 (1986).
[61] K. Ogusu, Opt. Quantum Electron. **19**, 65 (1987).
[62] N. N. Akhmediev, K. O. Boltar', and V. M. Eleonskiĭ, Opt. Spektrosk. **53**, 906 (1982) [Opt. Spectrosc. (USSR) **53**, 540 (1982)].
[63] N. N. Akhmediev, K. O. Boltar', and V. M. Eleonskiĭ, Opt. Spektrosk. **53**, 1097 (1982) [Opt. Spectrosc. (USSR) **53**, 654 (1982)].
[64] D. Mihalache *et al.*, Rev. Roum. Phys. **34**, 623 (1989).
[65] D. Mihalache *et al.*, Solid State Commun. **74**, 275 (1990).
[66] L. Fried, *Numerical Solution of Differential Equations* (Academic Press, New York, 1979).
[67] M. Gubbels *et al.*, Opt. Commun. **61**, 357 (1987).
[68] D. Mihalache and D. Mazilu, Rev. Roum. Phys. **34**, 493 (1988).
[69] D. Mihalache, D. Mazilu, M. Bertolotti, and C. Sibilia, J. Opt. Soc. Am. **B5**, 565 (1988).
[70] D. Mihalache, D. Mazilu, M. Bertolotti, and C. Sibilia, J. Mod. Opt. **35**, 1017 (1988).
[71] D. Mihalache and R. P. Wang, Phys. Lett. **132A**, 59 (1988).
[72] A. D. Boardman and P. Egan, IEEE J. Quantum Electron. **21**, 1701 (1985).
[73] C. T. Seaton *et al.*, IEEE J. Quantum Electron. **21** 774 (1985).
[74] A. S. Semenov, V. L. Smirnov, and A. V. Shmal'ko, *Integrated Optics for Information Transmission and Analysis Systems* [in Russian] (Radio i Svyaz', Moscow, 1990).

Translated by Julian B. Barbour